



CIVIL ENGINEERING STUDIES

Illinois Center for Transportation Series No. 20-023

UILU-ENG-2020-2023

ISSN: 0197-9191

Bridge Decks: Mitigation of Cracking and Increased Durability— Materials Solution (Phase III)

Prepared By

Robin Deb

Paramita Mondal

University of Delaware

Ardavan Ardeshirilajimi

University of Illinois at Urbana-Champaign

Research Report No. FHWA-ICT-20-016

A report of the findings of

ICT PROJECT R27-178-1

Bridge Decks: Mitigation of Shrinkage Cracking—Phase III

<https://doi.org/10.36501/0197-9191/20-023>

Illinois Center for Transportation

December 2020

TECHNICAL REPORT DOCUMENTATION PAGE

1. Report No. FHWA-ICT-20-016		2. Government Accession No. N/A		3. Recipient's Catalog No. N/A	
4. Title and Subtitle Bridge Decks: Mitigation of Cracking and Increased Durability—Materials Solution (Phase III)				5. Report Date December 2020	
				6. Performing Organization Code N/A	
7. Authors Robin Deb, Paramita Mondal, and Ardavan Ardeshirilajimi				8. Performing Organization Report No. ICT-20-023 UILU-2020-2023	
9. Performing Organization Name and Address Illinois Center for Transportation Department of Civil and Environmental Engineering University of Illinois at Urbana-Champaign 205 North Mathews Avenue, MC-250 Urbana, IL 61801				10. Work Unit No. N/A	
				11. Contract or Grant No. R27-178-1	
12. Sponsoring Agency Name and Address Illinois Department of Transportation (SPR) Bureau of Research 126 East Ash Street Springfield, IL 62704				13. Type of Report and Period Covered Final Report 9/15/17–12/15/20	
				14. Sponsoring Agency Code	
15. Supplementary Notes Conducted in cooperation with the U.S. Department of Transportation, Federal Highway Administration. https://doi.org/10.36501/0197-9191/20-023					
16. Abstract Type K cement offers a lower slump than conventional concrete, even at a higher water-to-cement ratio. Therefore, a suitable chemical admixture should be added to the Type K concrete mix design at a feasible dosage to achieve and retain target slump. In this project, a compatibility study was performed for Type K concrete with commercially available water-reducing and air-entraining admixtures. Slump and air content losses were measured over a period of 60 minutes after mixing and a particular mid-range water-reducing admixture was found to retain slump effectively. Furthermore, no significant difference in admixture interaction between conventional and Type K concrete was observed. Another concern regarding the use of Type K concrete is that its higher water-to-cement ratio can potentially lead to higher permeability and durability issues. This study also explored the effectiveness of presoaked lightweight aggregates in providing extra water for Type K hydration without increasing the water-to-cement ratio. Permeability of concrete was measured to validate that the use of presoaked lightweight aggregates can lower water adsorption in Type K concrete, enhancing its durability. Extensive data analysis was performed to link the small-scale material test results with a structural test performed at Saint Louis University. A consistent relation was established in most cases, validating the effectiveness of both testing methods in understanding the performance of proposed shrinkage-mitigation strategies. Stress analysis was performed to rank the mitigation strategies. Type K incorporation is reported to be the most effective method for shrinkage-related crack mitigation among the mixes tested in this study. The second-best choice is the use of Type K in combination with either presoaked lightweight aggregates or shrinkage-reducing admixtures. All mitigation strategies tested in this work were proved to be significantly better than using no mitigation strategy.					
17. Key Words Shrinkage, Bridge Deck, Cracking, Type K, Presoaked Lightweight Aggregates, Durability			18. Distribution Statement No restrictions. This document is available through the National Technical Information Service, Springfield, VA 22161.		
19. Security Classif. (of this report) Unclassified		20. Security Classif. (of this page) Unclassified		21. No. of Pages 45	22. Price N/A

ACKNOWLEDGMENT, DISCLAIMER, MANUFACTURERS' NAMES

This publication is based on the results of **ICT-R27-178-1: Bridge Decks: Mitigation of Shrinkage Cracking—Phase III**. ICT-R27-178-1 was conducted in cooperation with the Illinois Center for Transportation; the Illinois Department of Transportation; and the U.S. Department of Transportation, Federal Highway Administration.

Members of the Technical Review Panel (TRP) were the following:

- James Krstulovich, TRP Chair, Illinois Department of Transportation
- Hani Alnamer, Illinois Department of Transportation
- Julie Beran, Illinois Department of Transportation
- Dan Brydl, Federal Highway Administration
- Mike Copp, Illinois Department of Transportation
- Darrin Davis, Illinois Department of Transportation
- Kevin Riechers, Illinois Department of Transportation
- Megan Swanson, Illinois Department of Transportation
- Dan Tobias, Illinois Department of Transportation
- Melinda Winkelman, Illinois Department of Transportation
- Steve Worsfold, Illinois Department of Transportation

The contents of this report reflect the view of the authors, who are responsible for the facts and the accuracy of the data presented herein. The contents do not necessarily reflect the official views or policies of the Illinois Center for Transportation, the Illinois Department of Transportation, or the Federal Highway Administration. This report does not constitute a standard, specification, or regulation.

Trademark or manufacturers' names appear in this report only because they are considered essential to the object of this document and do not constitute an endorsement of product by the Federal Highway Administration, the Illinois Department of Transportation, or the Illinois Center for Transportation.

EXECUTIVE SUMMARY

Various shrinkage-mitigation strategies using Type K, presoaked lightweight aggregates (LWAs), and shrinkage-reducing admixtures (SRAs) were developed in the second phase of this project. The goal of this project is to verify their long-term effectiveness on concrete. Furthermore, the use of Type K cement needed further assessment in order to understand its effect on early-age properties (slump and air content) and durability before wider adoption for field application.

Because of rapid ettringite formation in concrete with Type K cement, Type K cement generally offers a lower slump than conventional concrete, even when a higher water-to-cement (w/c) ratio is used for proper hydration. Therefore, a suitable chemical admixture should be added to the Type K concrete mix design at a feasible dosage to achieve and retain target slump. In this project, a compatibility study was performed for Type K concrete with commercially available water-reducing and air-entraining admixtures. Slump and air content losses were measured over a period of 60 minutes after mixing. A particular mid-range water-reducing admixture retained slump effectively. Furthermore, no significant difference in admixture interaction between conventional and Type K concrete was observed.

Another concern regarding the use of Type K concrete is that its higher w/c ratio can potentially lead to higher permeability and durability issues. During the second phase of the project, the effectiveness of presoaked LWAs was explored to provide extra water for Type K hydration without increasing the w/c ratio. In this phase, the permeability of concrete was measured to validate that the use of presoaked LWAs can lower water adsorption in Type K concrete, enhancing its durability.

Effort was also made to verify the effectiveness of other shrinkage-mitigation strategies on concrete for a test duration of around six months. The negative impact of class C fly ash in reducing early-age expansion of Type K concrete was verified. Adding a small amount of external gypsum proved to be effective in counteracting the negative effect of class C fly ash.

Extensive data analysis was performed to link the small-scale material test results with a structural test performed at Saint Louis University. A consistent relation was established in most cases, validating the effectiveness of both testing methods in understanding the performance of the proposed shrinkage-mitigation strategies. Furthermore, stress analysis was performed to rank the mitigation strategies that show Type K incorporation as the most effective method for shrinkage-related crack mitigation among the mixes tested in this study. The second-best choice proved to be the use of Type K in combination with either presoaked LWAs or SRAs. Note that all mitigation strategies tested in this work proved to be significantly better than using no mitigation strategy.

TABLE OF CONTENTS

CHAPTER 1: INTRODUCTION	1
CHAPTER 2: EFFECTS OF TYPE K ON EARLY-AGE PROPERTIES AND ITS INTERACTION WITH CHEMICAL ADMIXTURES	3
MATERIALS AND METHODS	3
TEST RESULTS AND DISCUSSION	4
Compatibility of Admixtures with Control Mix	6
Compatibility of Admixtures with Type K Mix	7
Calorimetric Study of Type K Cement with Selected Admixtures.....	8
SUMMARY.....	9
CHAPTER 3: EFFECTS OF TYPE K ON DURABILITY OF CONCRETE	10
INTRODUCTION.....	10
MATERIALS AND METHODS	10
WATER ABSORPTION TEST	11
TEST RESULTS AND DISCUSSION	13
Comparison between Water-soaked and Air-dried Samples	13
SUMMARY.....	17
CHAPTER 4: LONG-TERM CONCRETE TESTING	18
MATERIALS.....	18
Raw Materials.....	18
Mixture Proportions	19
TEST METHODS	21
Mixing Procedure	21
Measuring Length Deformation of Concrete Samples.....	21
EFFECTS OF COMBINING LWA AND TYPE K CEMENT.....	22
VERIFYING THE NEED TO ADD EXTERNAL GYPSUM TO TYPE K CONCRETE WITH CLASS C FLY ASH	23
EFFECTS OF COMBINING SRA AND TYPE K FOR SHRINKAGE MITIGATION	26
SUMMARY.....	27

CHAPTER 5: LINKING LARGE- WITH SMALL-SCALE TEST RESULTS	29
EFFECTS OF RESTRAINT IN SMALL-SCALE TESTING	29
COMPARING LARGE- TO SMALL-SCALE STRAIN MEASUREMENTS	30
PERFORMANCE COMPARISON OF MIXES BASED ON TENSILE STRESS DEVELOPED AND CRACKING POTENTIAL.....	40
SUMMARY.....	41
CHAPTER 6: CONCLUSIONS	43
REFERENCES	44

LIST OF FIGURES

Figure 1. Photo. (a) Fresh concrete mix; (b) slump test setup; and (c) concrete kept in a mixing drum at 25 rpm to provide mild agitation and prevent stiffening.	4
Figure 2. Photo. (a) Fresh concrete mix; (b) Type A air meter; and (c) concrete kept in a mixing drum at 25 rpm to provide mild agitation and prevent stiffening.	4
Figure 3. Graph. Slump loss comparison between the control and Type K mixes.	5
Figure 4. Graph. Air content comparison between the control and Type K mixes.	5
Figure 5. Graph. Slump loss comparison between control, control+HRWRA, and control+MRWRA mixes. .	6
Figure 6. Graph. Slump retention comparison between control, control+HRWRA, and control+MRWRA mixes.	7
Figure 7. Graph. Slump loss comparison between Type K, Type K+HRWRA, and Type K+MRWRA.	7
Figure 8. Graph. Slump retention comparison between Type K, Type K+HRWRA, and Type K+MRWRA.	8
Figure 9. Graph. Heat evolution profiles for Type K, Type K+HRWRA, and Type K+MRWRA hydration process.	9
Figure 10. Graph. Slump value comparison of all mixes at 60 minutes.	9
Figure 11. Photo. Sample preparation steps for water absorption test.	11
Figure 12. Equation. Equations needed to calculate water absorption by concrete samples.	12
Figure 13. Photo. (a) Cross-sectional view, (b) 3D view, and (c) real-life picture of the experimental setup.	12
Figure 14. Graph. Comparison of absorption between control and Type K samples.	13
Figure 15. Graph. Absorption rate comparison between control and control+LWA (a) water-soaked and (b) air-dried samples.	14
Figure 16. Graph. Absorption rate comparison between Type K+LWA (a) water-soaked and (b) air-dried samples.	15
Figure 17. Graph. Absorption rate comparison between Type K+LWA+MRWRA (a) water-soaked and (b) air-dried samples.	16
Figure 18. Photo. A typical mold for restrained expansion in accordance with ASTM C878.	21
Figure 19. Graph. Effect of Type K+LWA on long-term unrestrained deformation of concrete.	22
Figure 20. Graph. Effect of Type K+LWA on long-term restrained deformation of concrete.	23
Figure 21. Graph. Effect of Type K+LWA on long-term unrestrained autogenous deformation of concrete.	23

Figure 22. Graph. Effect of external gypsum addition to Type K concrete with class C fly ash: long-term unrestrained deformation of concrete.	24
Figure 23. Graph. Effect of external gypsum addition to Type K concrete with class C fly ash: long-term restrained deformation of concrete.	25
Figure 24. Graph. Effect of external gypsum addition to Type K concrete with class C fly ash: long-term autogenous deformation of concrete.	25
Figure 25. Graph. Combining SRA with Type K: long-term unrestrained deformation of concrete.	26
Figure 26. Graph. Combining SRA with Type K: restrained deformation of concrete.	27
Figure 27. Graph. Combining SRA with Type K: unrestrained autogenous deformation of concrete. ...	27
Figure 28. Graph. Restrained-to-unrestrained shrinkage ratio.	30
Figure 29. Graph. Shrinkage measured in small-scale testing and large-scale model deck.	32
Figure 30. Graph. Ratio of shrinkage measured in small-scale testing and large-scale model deck.	33
Figure 31. Graph. Difference in shrinkage measured in small-scale testing and large-scale model deck.	35
Figure 32. Graph. Difference in expansion measured in small-scale testing and large-scale model deck.	37
Figure 33. Graph. Ratio of expansion measured in small-scale testing and large-scale model deck. ...	38
Figure 34. Graph. Difference in expansion measured in small-scale testing and large-scale model deck.	39

LIST OF TABLES

Table 1. Mix Designs for Workability Analysis	3
Table 2. Mix Designs for Durability Analysis	11
Table 3. Acronyms for Samples Used in the Water Absorption Test	13
Table 4. Chemical Composition of Raw Materials.....	18
Table 5. Phase Composition (%wt) of Raw Materials Obtained Using QXRD.....	19
Table 6. Mixture Proportions for Concrete Specimens with Fly Ash and Gypsum	20
Table 7. Mixture Proportions for Concrete Specimens with SRA	20
Table 8. Mixture Proportions for Concrete Specimens with LWA	20
Table 9. Stress Analysis for Type K	40
Table 10. Stress Analysis for Type K+LWA Mix.....	40
Table 11. Performance Ranking of Mixes at 28 days	41
Table 12. Performance Ranking of Mixes at 168 days.....	41

CHAPTER 1: INTRODUCTION

Durability is a key factor for concrete structures. A concrete bridge deck should sustain its required strength and serviceability during its lifetime. However, concrete decks with a large surface-to-volume ratio lead to significant drying shrinkage due to more exposed surfaces. Drying shrinkage forms transverse cracks, which may trigger further durability issues owing to reinforcement corrosion, freeze thaw, and an alkali-silica reaction (also known as “concrete cancer”) caused by intrusion of deicing salts and harmful chemicals in concrete (Mehta 1999; Neville 2001).

The ACI Committee (2010) have recommended several strategies that can help curtail shrinkage in concrete. These strategies include the use of shrinkage-reducing admixtures and supplemental cementitious materials such as pozzolans, expansive additives, etc. The first phase of this study developed different concrete mix designs and used expansive additives to curb shrinkage (Chaunsali et al. 2013). The researchers concluded that the use of a calcium sulfoaluminate (CSA) cement, marketed as “Komponent,” at a 15% replacement of ordinary Portland cement (OPC) to develop a Type K (85% OPC + 15% CSA) cement can effectively compensate for the drying shrinkage problem in laboratory conditions. In the second phase of this study, Ardeshirilajimi et al. (2016) found that a combination of Type K cement and lightweight aggregates (LWAs) in mortar mixes were beneficial against autogenous and drying shrinkage. By using presoaked LWAs, internal curing can be achieved during hydration of unreacted cementitious particles. When the relative humidity falls below a critical level due to self-desiccation and evaporation, LWAs release the required amount of water to replace the lost moisture and facilitate hydration. This mechanism helps to prevent early cracking and ingress of aggressive chemicals as well as reduces porosity and improves durability at later ages (Bentz and Weiss 2011).

Even though Type K concrete proved to be effective in shrinkage mitigation, a holistic study was necessary to understand its effect on durability and early-age properties. Because the Type K mix has a higher water-to-cement (w/c) ratio than the conventional concrete mix used in bridge decks, concrete made with Type K can have a higher susceptibility to developing a porous microstructure than the latter. Type K concrete exhibited more rapid slump loss than the OPC concrete mix, which adversely affects workability during transportation and construction. To tackle the workability issues and ease of construction, engineers have been using chemical admixtures/superplasticizers in fresh concrete for the last 50 years. Some benefits of using chemical admixtures are improved workability in fresh concrete as well as increased strength and durability due to the limited formation of capillary pores, which results in less permeability in hardened concrete (Collepardi 2005). However, few studies have been performed to understand the interaction between chemical admixtures and expansive cement. Fu et al. (1995) found that admixtures based on sodium sulfonated naphthalene formaldehyde and sodium sulfonated melamine formaldehyde in combination with pre-hydrated high alumina cement helped early-age formation of ettringite, reducing late-age expansion and preventing unwanted damage to hardened concrete. On another note, some traditional chemical admixtures hindered early-age formation of ettringite up to a certain degree, which led to dosage optimization for future purposes.

The objective of this study was to understand workability and durability issues associated with Type K concrete and provide feasible solutions. In this study, different commercially available chemical admixtures were incorporated into concrete mix designs to determine slump and air content losses. Then, hardened concrete samples were prepared to investigate durability properties by measuring the degree of water absorption.

Another objective of this study was to verify the effectiveness of the shrinkage-mitigation strategies developed in the second phase of the project using mortar mixes in concrete (Ardeshirilajimi et al. 2016). Long-term testing of small-scale concrete samples was performed during this phase, and effort was made to link the results with the structural testing performed at Saint Louis University (Rahman et al. 2020). During the previous phases of this project, the expansion and shrinkage strains measured during small-scale testing were always significantly higher compared to the strains measured at a large scale. Extensive data analysis was performed as part of this study to link test results from two different length scales.

It was difficult to compare overall performance between mixes, as shrinkage mitigation was achieved using fundamentally different mechanisms: early-age expansion for any mix with Type K versus reduction of shrinkage in mixes with SRAs or presoaked LWAs. Therefore, stress analysis was performed based on the structural testing results and small-scale free shrinkage measurements to rank mixes based on their performance in mitigating cracking due to shrinkage.

CHAPTER 2: EFFECTS OF TYPE K ON EARLY-AGE PROPERTIES AND ITS INTERACTION WITH CHEMICAL ADMIXTURES

This chapter explores if there are any adverse interactions between Type K concrete and chemical admixtures commonly used in concrete. At early age, Type K hydrates rapidly to form ettringite, which can lead to a high degree of heat evolution and rapid use of water (Huang et al. 2019). As a result, concrete made from Type K cement should hypothetically have a shorter setting time than conventional OPC concrete, which can make pouring, dispersing, and finishing difficult. However, the use of chemical admixtures at optimal dosages can potentially offset this behavior. Therefore, research reported herein was intended to determine if there is any discrepancy between the behavior of conventional concrete versus Type K concrete in the presence of water-reducing and air-entraining admixtures. This chapter summarizes the slump loss and air content tests. After trial and error as well as discussion with the Type K provider (CTS cement), two polycarboxylate (PCE)-based admixtures were selected for this study. The dosages of these admixtures were kept to a minimum and behavior between conventional OPC concrete and Type K concrete was compared, as admixture dosage optimization was beyond the scope of this work.

MATERIALS AND METHODS

To investigate the slump and air content losses, slump tests (ASTM 2015) and air content tests (ASTM 2010) were performed on the concrete mixes shown in Table 1. The tests were performed initially for 60 minutes at 15-minute intervals from time “zero,” the time when concrete mixing was finished. Figure 1 and Figure 2 show the experimental procedure used.

Table 1. Mix Designs for Workability Analysis

Mix Design	Acronym	OPC (lb/yd ³)	CSA (lb/yd ³)	FA (lb/yd ³)	CA (lb/yd ³)	Water (lb/yd ³)	Water-cement ratio	AEA ¹ (fl oz/cwt)
Control	C	610		1,130	1,826	268	0.44	2
Control+HRWRA ²	CHR	610		1,130	1,826	268	0.44	2
Control+MRWRA ³	CMR	610		1,130	1,826	268	0.44	2
Type K ⁴	K	519	91	1,130	1,826	299	0.49	2
Type K+HRWRA	KHR	519	91	1,130	1,826	299	0.49	2
Type K+MRWRA	KMR	519	91	1,130	1,826	299	0.49	2

AEA¹—MasterAir AE200

HRWRA²—MasterGlenium 3400 dosage at 2 fl oz/cwt

MRWRA³—MasterPolyheed 1020 dosage at 3 fl oz/cwt

Type K⁴—85% OPC + 15% CSA

Each batch of concrete mix weighing in at around 60 lb (0.42ft³ in volume) was prepared by conforming to the standards of ASTM C685 (ASTM 2001). For the slump loss test, the concrete was dumped back into the mixer after every measurement for two reasons. First, the mixer drum kept rotating at 25 revolutions per minute (rpm), which allowed mild agitation of the concrete and prevented stiffening. The second reason was to simulate field conditions, as concrete during delivery and placement is kept in a mixer that continuously provides mild agitation.

Compared to the slump loss testing method, concrete was discarded after every successive air content measurement. A small amount of water was added to measure air content using the pressure method, which changes the water content of the fresh concrete slightly. Therefore, reusing the same concrete will introduce inconsistency during successive testing. To eliminate such complications, more than 100 lb (0.69 ft³ in volume) of fresh concrete had to be produced for the air content test for a single investigation.

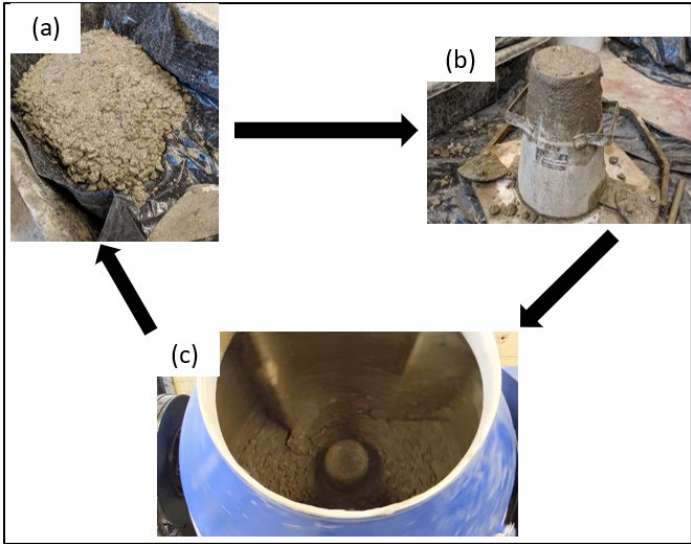


Figure 1. Photo. (a) Fresh concrete mix; (b) slump test setup; and (c) concrete kept in a mixing drum at 25 rpm to provide mild agitation and prevent stiffening.

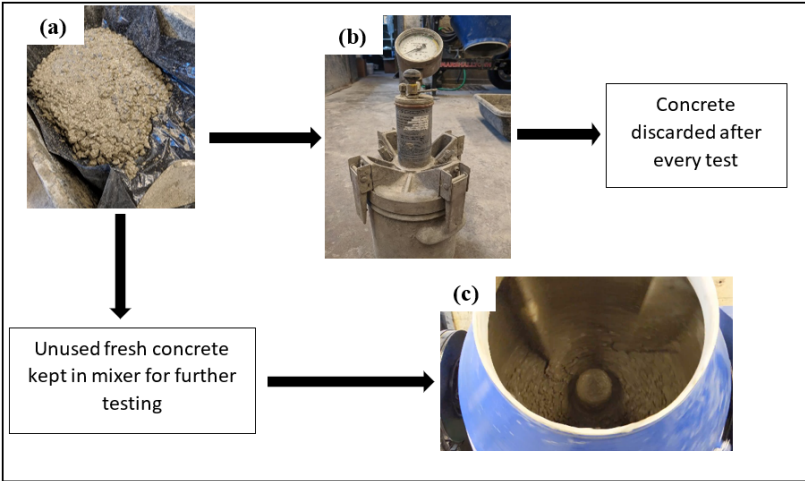


Figure 2. Photo. (a) Fresh concrete mix; (b) Type A air meter; and (c) concrete kept in a mixing drum at 25 rpm to provide mild agitation and prevent stiffening.

TEST RESULTS AND DISCUSSION

To validate a hypothesis that Type K concrete (referred to as “K”) offers poorer workability than conventional concrete, slump and air content tests were conducted initially using a K mix and a

conventional concrete (“C”) mix. Figure 3 and Figure 4 compare the slump and air content measurements, respectively, for two mix designs. Slump and air content losses for K mix were consistently higher than those of C mix. Even though the water-to-cement ratio for K mix was 0.49 and had the same dosage of an air-entraining agent as C mix, the slump and air content values at time zero were 13.7% and 28.2% lower, respectively, for K mix than C mix. However, the difference in percentages between the measurements remained consistent throughout the 60-minute observation period. Based on the data, K mix shows a higher need for chemical admixtures to achieve early-age properties suitable for construction purposes. However, it was encouraging to see the difference in behavior between the two concretes remained consistent with time.

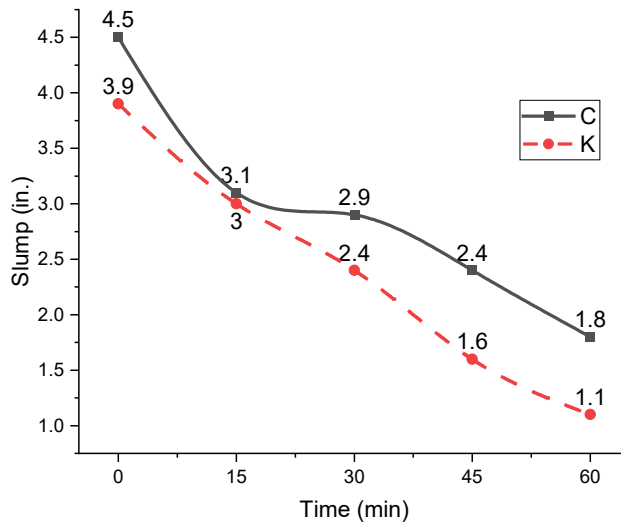


Figure 3. Graph. Slump loss comparison between the control and Type K mixes.

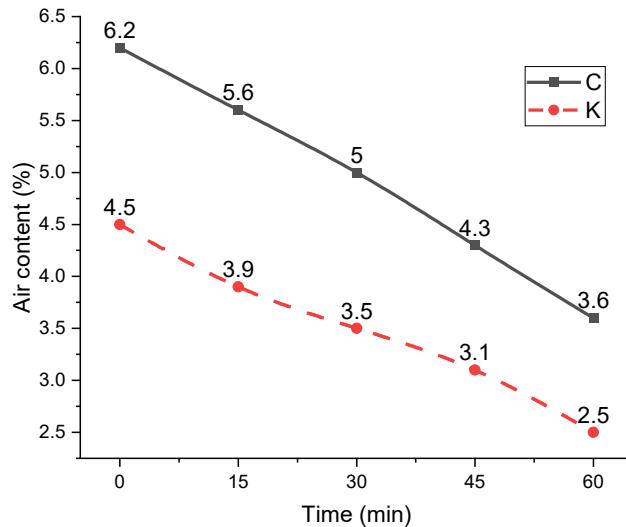


Figure 4. Graph. Air content comparison between the control and Type K mixes.

After experimentation with a few trial batches, one mid-range water-reducing admixture (MRWRA), MasterPolyheed 1020, and one high-range water-reducing admixture (HRWRA), MasterGlenium 3400, which are commercially produced by BASF®, were selected for use in the concrete mixes. The

main objective of this work was to investigate if Type K concrete interferes with chemical admixtures or has any unexpected compatibility issues compared to conventional concrete.

Compatibility of Admixtures with Control Mix

To establish the baseline behavior for the control mix, slump loss tests were first performed using Control (C), Control+HRWRA (CHR), and Control+MRWRA (CMR) mixes and plotted against the target (TGT) value at 4 in. for standard comparison. In Figure 5, the slump value for C goes below 4 in. around 10 minutes after mixing. In contrast, the slump values for CHR and CMR go below the target approximately 35 minutes after mixing. These observations show the effectiveness of the admixtures with the conventional mix. At time zero, the slump values for CHR and CMR were 30.6% and 50%, respectively, compared to the C mix. Similarly, at the end of 60 minutes, the slump values for CHR and CMR were 64.6% higher compared to C mix. Even though all mixes had the same w/c ratio, the admixtures significantly improved the workability characteristics throughout the testing period of 60 minutes. According to the product distributors, both selected admixtures contain a similar cement dispersant, which are based on polycarboxylate groups. Both chemical admixtures are manufactured using a free radical polymerization process involving a variety of organic monomers, among which ether and carboxylic acid monomers are significant. Both chemistries seemed to provide consistent results when used with conventional concrete.

One difference between the two admixtures is their effect at time zero. Figure 5 and Figure 6 (which shows the percentage difference from the target 4 in. slump) show the mid-range water reducer was more effective in increasing the early-age slump than the high range. This is interesting because the fundamental difference between MRWRA and HRWRA is the amount of water content reduction they can offer. MRWRA can reduce water content up to 10%, while HRWRA can reduce water content from 12% to 40% (Day et al. 2013). But, in this case, the slump values for CMR were higher compared to CHR until 35 minutes after mixing. The contradiction possibly is due to the higher dosage of MRWRA used in this study (3 fl oz/cwt) compared to the HRWRA dosage (2 fl oz/cwt), both of which are the minimum recommended dosage by the provider.

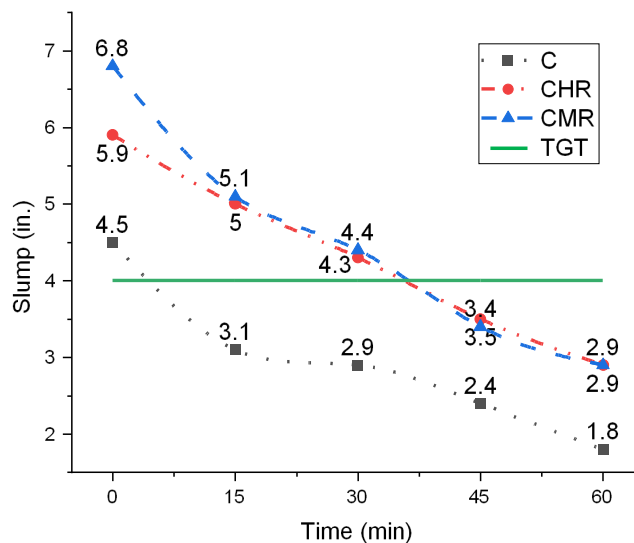


Figure 5. Graph. Slump loss comparison between control, control+HRWRA, and control+MRWRA mixes.

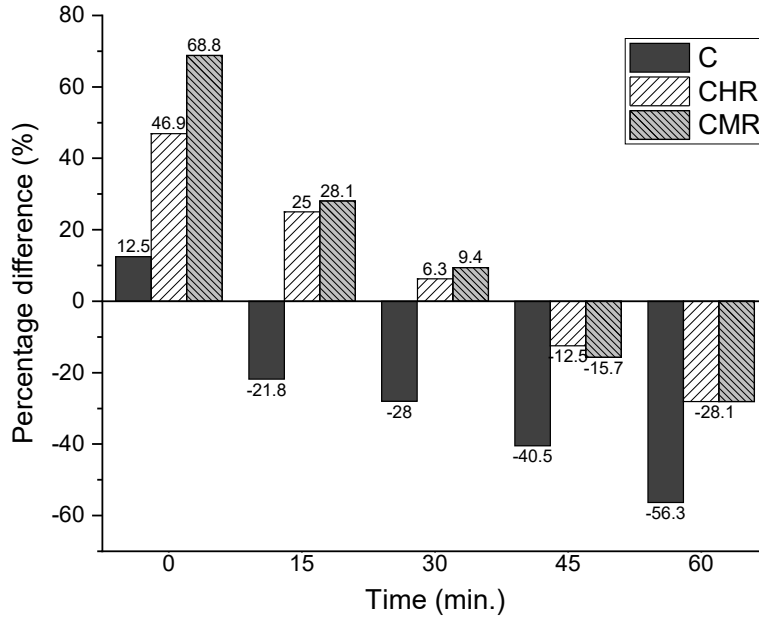


Figure 6. Graph. Slump retention comparison between control, control+HRWRA, and control+MRWRA mixes.

Compatibility of Admixtures with Type K Mix

Once the effectiveness of the chemical admixtures for the control mix was established, the slump retention capabilities of selected agents with the Type K mix were observed. Two mixes were designed: Type K+HRWRA and Type K+MRWRA. Figure 7 juxtaposes the results of slump loss with the target value of 4 in., and Figure 8 compares the percentage differences.

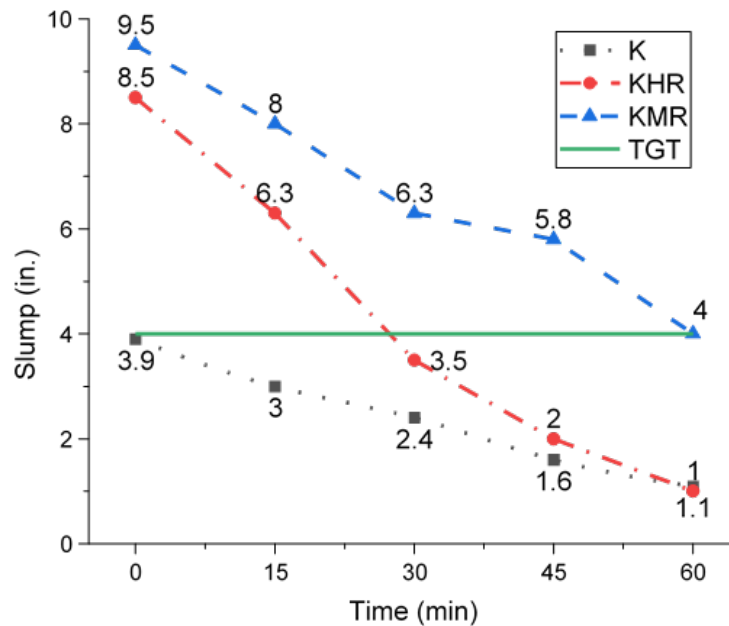


Figure 7. Graph. Slump loss comparison between Type K, Type K+HRWRA, and Type K+MRWRA.

Both admixtures had a positive impact in improving workability of the Type K mix. The slump at time zero was 132% higher for the high-range water reducer (KHR) than K mix. While the slump values remained consistently higher for KHR, the difference of slump values became smaller as time approached 60 minutes. At the end of 60 minutes, the slump value was 1.1 in., which is only 10% more than the K mix. In contrast, the initial slump for the mid-range water reducer (KMR) was 177% higher than the K mix. Similarly, the difference of slump values remained consistently higher until the end of 60 minutes. At the end of 60 minutes, the slump for KMR was 4 in., which is an approximately 250% increase compared to the slump value for K mix at 60 minutes.

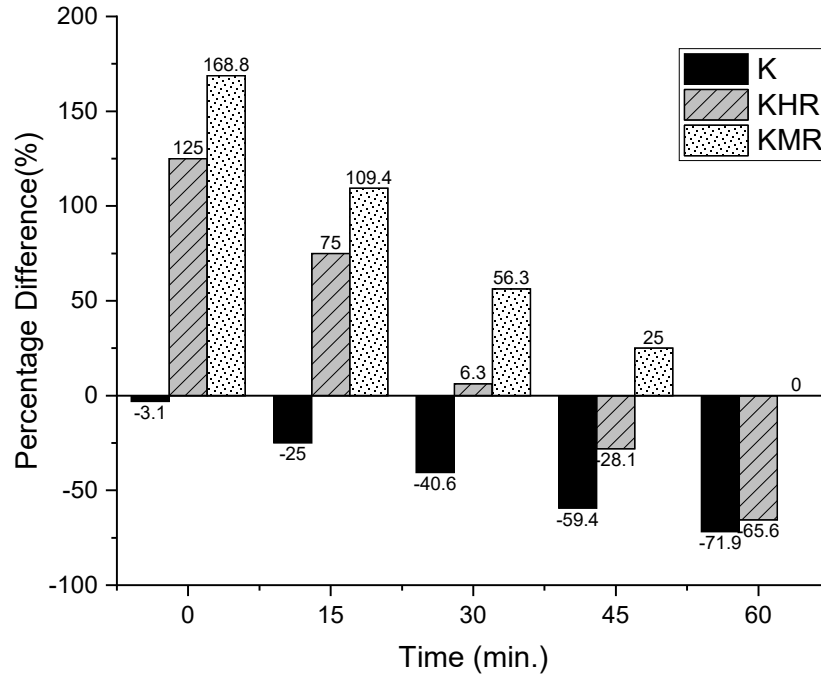


Figure 8. Graph. Slump retention comparison between Type K, Type K+HRWRA, and Type K+MRWRA.

Calorimetric Study of Type K Cement with Selected Admixtures

To understand the retardation effect of the admixtures, a calorimetric study was done with three different samples (K, KMR, KHR). The materials were proportioned according to the mix designs, and the mixing was done as follows: (i) mix OPC and CSA cement for fine distribution; (ii) add water with admixture, if specified; and (iii) prepare samples by uniform mixing and proper placement inside ampoules before putting them inside the calorimeter at 25°C. Heat evolution data was collected for 24 hours and presented in Figure 9. Observations show that the Type K hydration process is rapid and starts setting at the lowest time compared to KMR and KHR heat profiles. Additionally, the heat evolution of KMR is subdued in comparison to the KHR heat profile. This justifies the observation with slump loss values and also proves that the MRWRA retardation keeps Type K hydration at a dormant period for the longest period of time. As a result, the KMR values stay at a lower viscous phase, which will help to retain slump and ensure proper placement during construction.

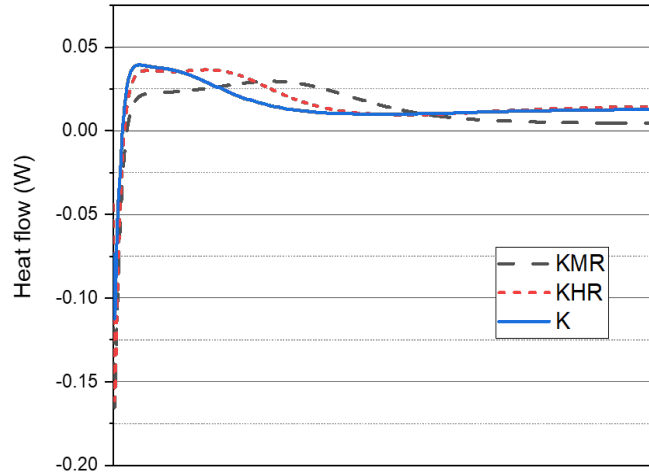


Figure 9. Graph. Heat evolution profiles for Type K, Type K+HRWRA, and Type K+MRWRA hydration process.

SUMMARY

In conclusion, a mid-range water reducer worked better than a high-range water reducer in both the control and Type K concrete mixes. This observation can be affected by the difference in dosage and molecular structure of the admixture. In addition to having the highest initial fluidity after mixing, the Type K mix with a mid-range water-reducing admixture had a 4" slump after 60 minutes (Figure 10). Some studies have found that fluidity retention is directly related with the molecular structure of the admixture used. It is possible that this particular mid-range water-reducing admixture had a higher number of carboxyl groups attached to the molecular structure, which facilitated better slump retention by keeping the hydration mechanism at a dormant phase for a more extended period of time. Moreover, no drastic difference in the admixture interaction between the control and Type K mixes were observed. This is a positive sign to consider while performing admixture dosage optimization of Type K concrete mixes for field implementation.

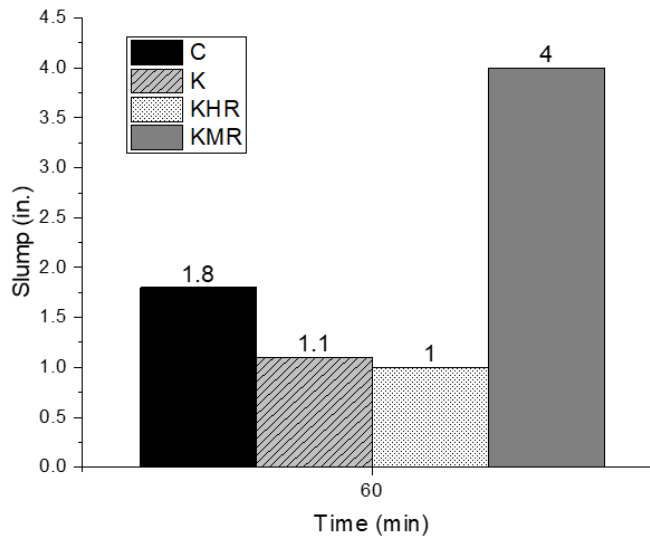


Figure 10. Graph. Slump value comparison of all mixes at 60 minutes.

CHAPTER 3: EFFECTS OF TYPE K ON DURABILITY OF CONCRETE

INTRODUCTION

Concrete was once regarded as a durable construction material requiring minimal inspection and maintenance (Sabir, Wild, and O'Farrell 1998). However, over the past few decades, many degradation mechanisms have been established that decrease the lifespan of concrete structures. Concrete on highway bridges is exposed to a repetitive wetting and drying process due to variable weather conditions (Sabir, Wild, and O'Farrell 1998). These fluctuating weather conditions influence the transport of water and other agents through capillary pores, which influence long-term performance of concrete; water ingress in concrete either facilitates freeze-thaw damage in cold weather or acts as a medium for harmful ions (chloride, sulfate, etc.) (Yang, Weiss, and Olek 2006).

One of the concerns in using Type K concrete for construction is its higher water content, which can possibly lead to increased durability issues. During the second phase of this study, the use of presoaked LWAs proved to be an effective method to provide extra water for Type K hydration, reducing the free water content in the concrete (Ardeshirilajimi et al. 2016). This chapter reports a durability study to understand the effects of Type K incorporation and Type K+LWA combination.

This chapter focuses on measuring water ingress in concrete, because most durability concerns in concrete come from water ingress. Transport of water through cementitious materials occurs in three methods: permeability, diffusion, and absorption. Absorption of water in concrete is generally governed by the capillary suction near the unsaturated concrete surface, and this process is comparatively faster than general diffusion or capillary absorption (Martys and Ferraris 1997). The water absorption test of concrete demonstrates a degree of durability of the concrete used to build structures in aggressive environments. To determine the water transport mechanisms in cementitious materials, three approaches have been established: experimental, numerical simulation, and analytical (Wang 2009). The most dominant and accurate approach is the experimental method, where methods such as nuclear magnetic resonance, gamma rays, etc. can be used to observe the dynamic mechanism of water transport through the concrete's capillary pores. However, these methods are too expensive and, as a result, the gravimetric method is currently the most widespread (Goual et al. 2000). In the gravimetric method, preconditioned concrete samples with variable relative humidity allow water ingress through the exposed surfaces.

MATERIALS AND METHODS

Table 2 presents the mix proportions used for sample preparation. The 24-hour absorption capacity of LWAs was found to be 16.83% by using ASTM C128 standard specifications (ASTM 2004). LWAs were presoaked for 24 hours prior to mixing. For each mix design, four 4" × 8" concrete cylinders (32 in total) were prepared following ASTM C192 standards (ASTM 2007). After each casting session, fresh samples were kept in a temperature-controlled room for 24 hours before demolding. Later, these samples were submerged underwater for curing purposes. Samples that were selected for the water absorption test were cured for 14 days, and samples selected for the compressive strength test were cured for 28 days.

Table 2. Mix Designs for Durability Analysis

Mix Design	Acronym	OPC (lb/yd ³)	CSA (lb/yd ³)	FA (lb/yd ³)	CA (lb/yd ³)	Free water-cement ratio	Water fed by LWA (lb/yd ³)	Total water cement ratio
Control	C	610		1,130	1,826	0.44	0	0.44
Control+LWA (35%)	CL35	610		1,130	1,826	0.33	67	0.44
Control+LWA (17%)	CL17	610		1,130	1,826	0.386	33.5	0.44
Type K ²	K	519	91	1,130	1,826	0.49	0	0.49
Type K ² +LWA (35%)	KL35	519	91	1,130	1,826	0.381	67	0.49
Type K ² +LWA (17%)	K17	519	91	1,130	1,826	0.437	33.5	0.49
Type K ² +LWA (35%)+ MRWRA ³	K35MR	519	91	1,130	1,826	0.381	67	0.49
Type K ² +LWA (17%)+MRWRA ³	K17MR	519	91	1,130	1,826	0.437	33.5	0.49

AEA¹—MasterAir AE200 dosage at 2 fl oz/cwt

Type K²—85% OPC + 15% CSA

MRWRA³—MasterPolyheed 1020 dosage at 3 fl oz/cwt

WATER ABSORPTION TEST

Sorptivity is widely accepted as the measure of the degree of saturation to characterize the water transport property through different concrete samples (Neithalath 2006). To perform this test, guidelines from ASTM C642, C1585, and C1757 (ASTM 1997, 2013, 2014) were followed to design the experiment. For each mix design, two 4" × 8" cylinders were casted and cured for 14 days. Later, the cylinders were cut into 4" × 2" using a saw. Three discs were obtained from each cylinder (six for each mix design). Every two discs went through a specific sample conditioning; this step is critical because water absorption rate is responsive to moisture content of the concrete sample (Parrott 1994). As a result, two sample conditionings were used for this test: water soaked (WS) and air dried (AD). Figure 11 illustrates the critical sample conditioning steps.

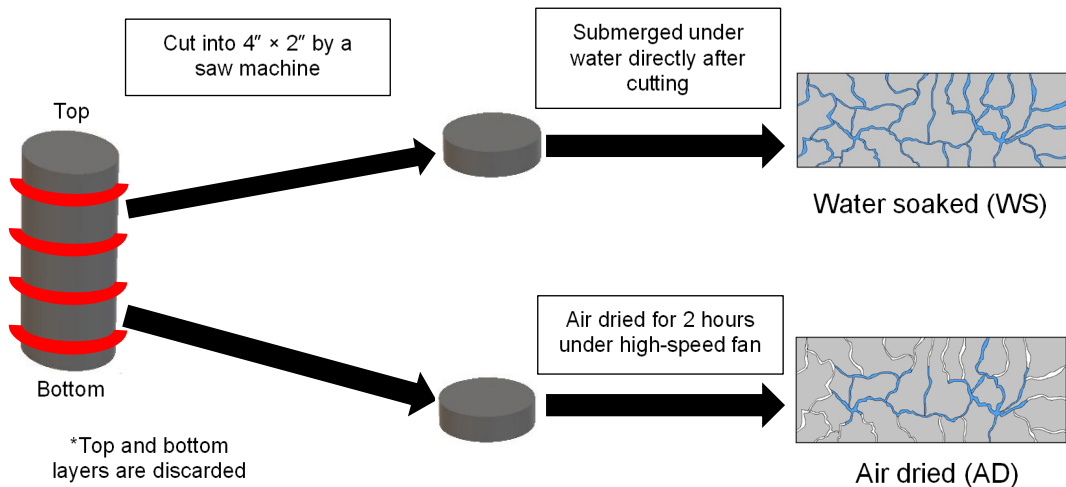


Figure 11. Photo. Sample preparation steps for water absorption test.

The WS and AD samples were submerged underwater immediately after sample conditioning. To get the degree of saturation for each sample, the following formulas were adopted. The change in mass is divided by the total surface area of the specimen, as shown in Figure 12 below:

$$\text{Absorption(g/mm}^2\text{)} = \frac{\Delta \text{ mass}}{\text{Surface area}}$$

$$\Delta \text{ mass(g)} = (\text{mass at } t^{\text{th}} \text{ time}) - (\text{mass at time 'zero'})$$

$$\text{Surface area(mm}^2\text{)} = 2 * \pi * r^2 + 2 * \pi * r * h$$

Figure 12. Equation. Equations needed to calculate water absorption by concrete samples.

In this investigation, water uptake was simulated throughout the exposed surface area of the concrete discs. After submerging each disc at time zero, mass readings were taken every 30 minutes for 4 hours to measure initial rapid absorption. Then, the mass readings for each disc were taken every 24 hours for 7 days. This step is important because concrete with Type K, chemical admixtures, and LWAs tend to behave differently than conventional OPC samples. In several earlier studies, presoaked LWA provided internal curing for late-age hydration of cement particles. As a result, depercolation/disconnection effects can be observed, which reduce capillary porosity in the concrete microstructure (Powers 1959). This can be categorized as self-healing—the process by which a material recovers itself from sustained damage and gains an improvement on its performance (De Rooij et al. 2013). In addition, studies have also found that partial replacement of OPC cement with Type K (or CSA expansive cement) helped with self-healing properties and improved durability (Hosoda 2007; Sisomphon and Copuroglu 2010). Based on these conclusions, the Type K samples with added LWAs and MRWRA are expected to perform better than control samples. Figure 13 represents the experimental setup.

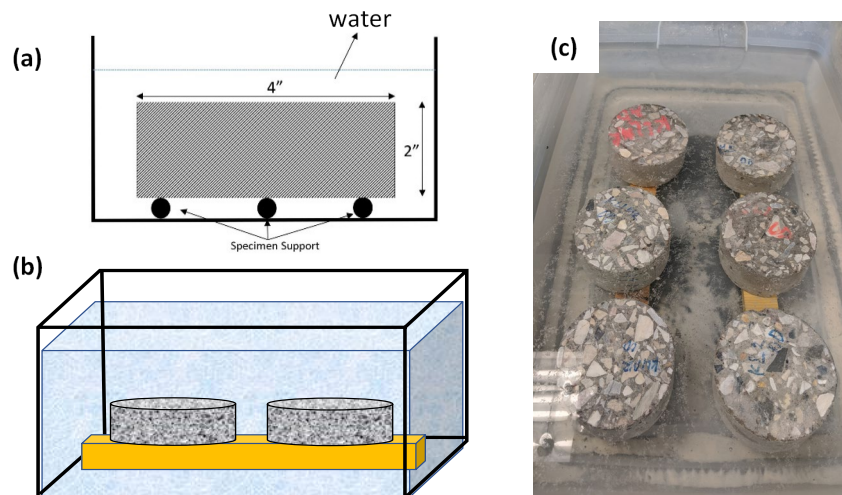


Figure 13. Photo. (a) Cross-sectional view, (b) 3D view, and (c) real-life picture of the experimental setup.

TEST RESULTS AND DISCUSSION

Table 3 lists the acronyms for the samples prepared for this investigation.

Table 3. Acronyms for Samples Used in the Water Absorption Test

Mix Design	Short Form	Water Saturated	Air Dried
Control	C	C_WS	C_AD
Control + 35% LWA	CL35	CL35_WS	CL35_AD
Control + 17% LWA	CL17	CL17_WS	CL17_AD
Type K	K	K_WS	K_AD
Type K + 35% LWA	KL35	KL35_WS	KL35_AD
Type K + 17% LWA	K17	KL17_WS	KL17_AD
Type K + 35% LWA +MRWRA	KL35MR	KL35MR_WS	KL35MR_AD
Type K + 17% LWA +MRWRA	KL17MR	KL17MR_WS	KL17MR_AD

Comparison between Water-soaked and Air-dried Samples

The absorption rate for C and K samples were plotted against the square root of time (Figure 14). The air-dried samples had a higher absorption rate than water-saturated samples. Because of the drying effect, AD samples had a lower relative humidity than WS samples. Moreover, although K samples were touted to have a denser microstructure, that was not the case. Instead, the K samples absorbed more water than the C samples in both water-soaked and air-dried conditions. At the end of seven days, the absorption for K_WS was 45% more compared to C_WS. Similarly, the difference between K_AD and C_AD at the end of seven days was almost 50%. Based on these observations, it seems that concrete made from Type K will perform poorly against aggressive environments. There can be a multitude of reasons behind this observation. The Type K sample had a higher w/c ratio (0.49) than the C sample (0.44). However, one caveat to that explanation is that ettringite is known to absorb water due to incomplete hydration of ye'elimite particles. This may introduce some errors in the measurement and can result in higher observed water absorption in the Type K samples.

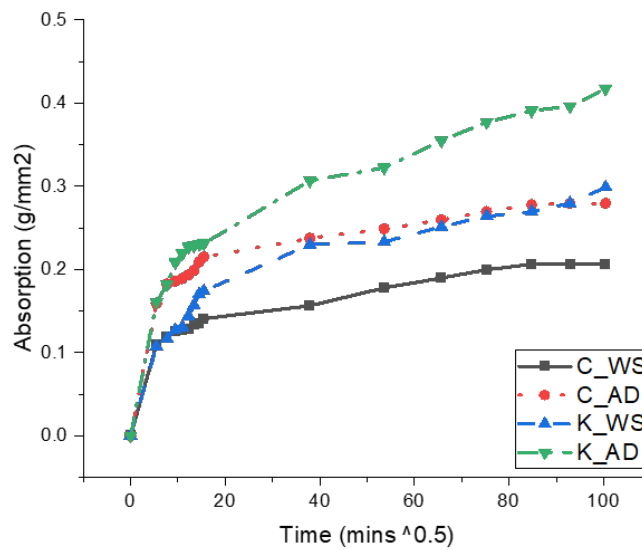
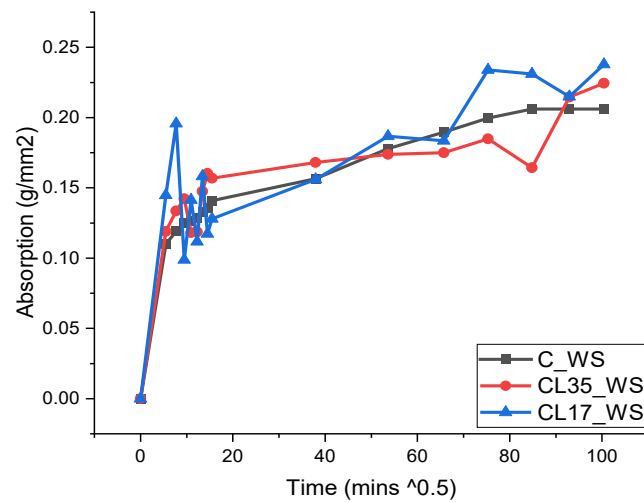


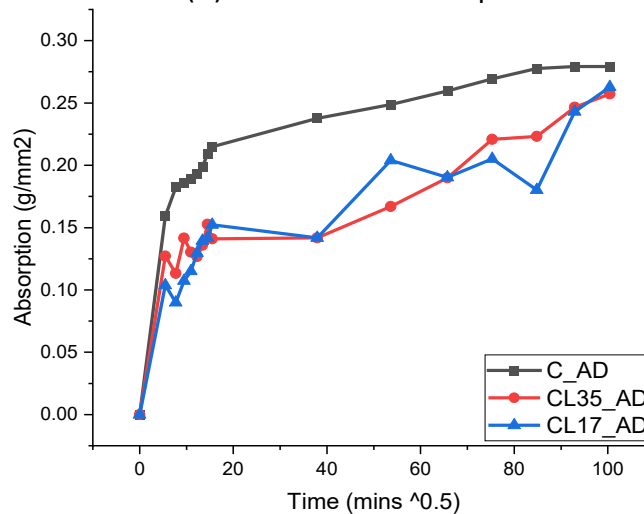
Figure 14. Graph. Comparison of absorption between control and Type K samples.

Before Type K+LWA mixes are tested, the effect of adding LWAs to conventional concrete is first tested using two mix designs, CL35 (35% replacement of fine aggregates with LWAs) and CL17 (17% replacement of fine aggregates with LWAs), to explore the benefits of internal curing. In Figure 15, a direct comparison between C, CL35, and CL17 was drawn to illustrate the absorption rate differences.

As presented in Figure 15, the addition of LWAs did not cause any significant difference in the water absorption of conventional concrete when the concrete was wet before testing. In the second phase of this experiment, air-dried and water-soaked samples were tested to compare the effect of LWAs under an elevated drying condition (Ardeshirilajimi et al. 2016). In Figure 15-B, C, CL35, and CL17 absorption data under air-drying preconditioning were juxtaposed. In this case, for both CL35_AD and CL17_AD samples (8% and 4%, respectively), the absorption capacities after seven days were significantly lower than those of C_AD samples.



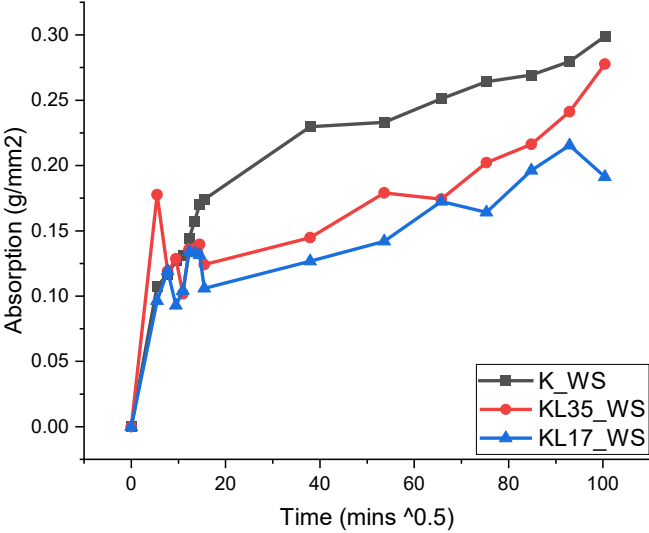
(A) Water-soaked samples



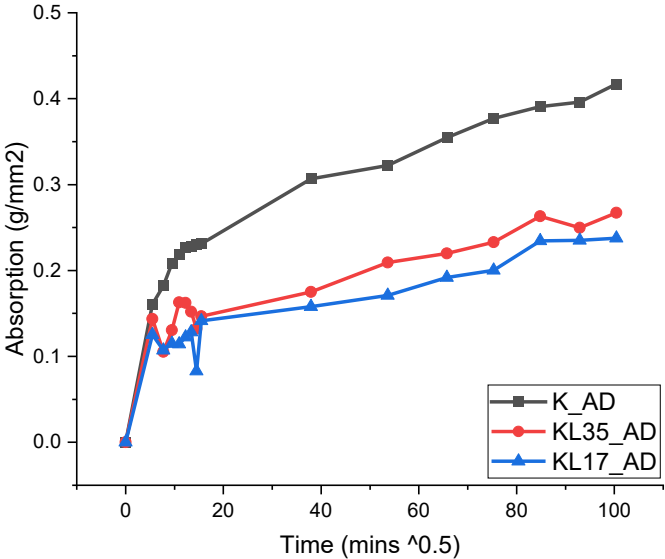
(B) Air-dried samples

Figure 15. Graph. Absorption rate comparison between control and control+LWA (a) water-soaked and (b) air-dried samples.

Later, the investigation was geared toward observing the effects of internal curing in Type K concrete samples. For this part, two mix designs were prepared: KL35 (35% replacement of fine aggregates with LWAs) and KL17 (17% replacement of fine aggregates with LWAs). Water absorption data for K, KL35, and KL17 were plotted in Figure 16 to draw a contrast between performance and water ingress. Samples with LWAs performed significantly better at reducing water absorption. At the end of seven days, the water absorption for KL35_WS was 7% lower than K_WS. In contrast, KL17_WS water absorption was 36% lower than K_WS. The absorption for KL17_WS was more than 7% lower than C_WS at the end of seven days. For air-dried samples, the water absorption for KL35 and KL17 drastically decreased.



(A) Water-soaked samples

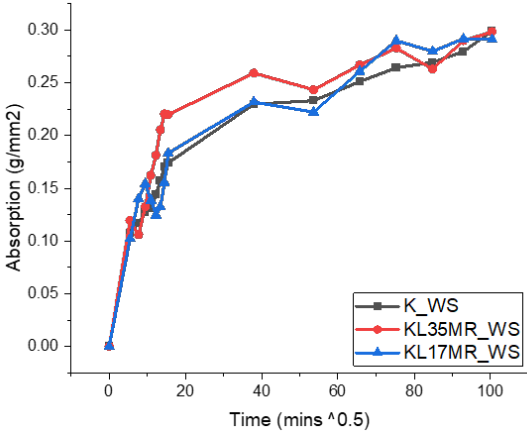


(B) Air-dried samples

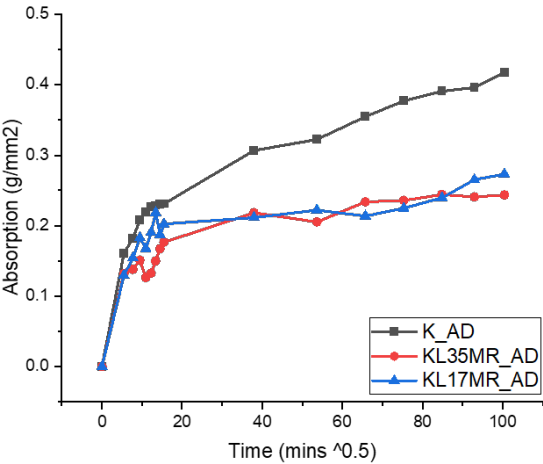
Figure 16. Graph. Absorption rate comparison between Type K+LWA (a) water-soaked and (b) air-dried samples.

The main concern of using admixtures is the delayed formation of ettringite (Taylor, Famy, and Scrivener 2001), which cause microcrack formation on matured concrete. As a result, concrete samples become susceptible to water ingress and demonstrate reduced durability properties. However, incorporation of presoaked LWAs in concrete volume allow cement hydration of cement particles due to internal curing, thereby allowing calcium carbonate precipitates to be deposited at the cracks, which can be classified as a self-healing mechanism.

Figure 17-A and Figure 17-B illustrate the water absorption capacity of K, KL17MR, and KL35MR concrete samples. From the initial interpretation of data patterns, the impact of air-drying concrete samples can be correlated with reduced water absorption after seven days. In contrast, water-soaked samples had almost the same water absorption after seven days. Air drying of concrete samples reduced the internal relative humidity, which triggered water release from the presoaked LWAs. As a result, unhydrated cement particles received water, which caused late-age reactions and formed a denser microstructure. In Figure 17-B, it can be observed that KL35MR_AD samples had the lowest water absorption after seven days. In fact, the absorption value was 67% lower than K_AD.



(A) Water-soaked samples



(B) Air-dried samples

Figure 17. Graph. Absorption rate comparison between Type K+LWA+MRWRA (a) water-soaked and (b) air-dried samples.

SUMMARY

LWAs made an impact in reducing water absorption of Type K concrete samples. This can be attributed towards the internal curing mechanism offered by presoaked LWAs. During curing procedures, LWAs offer additional water for hydration of Type K. This eliminates the need for using a higher water-to-cement ratio in Type K concrete, which tends to negatively affect concrete permeability and durability. In fact, in comparison to the C_AD water absorption value after seven days, KL35MR_AD was 24% lower. Based on these percentage comparisons, the choice of using KL35MR mix design for bridge decks would be prudent. As bridge decks after casting experience mild to severe drying conditions, the incorporation of presoaked LWAs in mix design can help counteract the incomplete hydration of cement particles and form a denser microstructure at a late age. Additionally, LWAs reduce the free water-to-cement ratio, which can help the concrete to attain more compressive strength compared to Type K concrete.

CHAPTER 4: LONG-TERM CONCRETE TESTING

During the second phase of this project, several shrinkage-mitigation strategies showed promise when tested at the small-scale using mortar samples (Ardeshirilajimi et al. 2016). One of the primary objectives of this phase was to verify if the same strategies affect concrete long term. This chapter reports long-term test results of concrete samples using various shrinkage-mitigation strategies. This part of the project was performed at the concrete lab at the University of Illinois's Newmark Civil Engineering Laboratory.

MATERIALS

Raw Materials

Type I Portland cement (from Essroc Co.) and a commercially available CSA cement (sold as KSC Komponent by CTS Cement) were used in this study. Quantitative X-ray diffraction (QXRD) analysis was performed to determine the mineralogical composition of OPC and CSA cement as well as fly ash. Table 4 shows the oxide composition of all raw materials. The phase composition of raw materials was determined using QXRD analysis and is given in Table 5. Natural sand (fine aggregate, FA 1 based on IDOT specification) with a specific gravity of 2.6, fineness modulus of 2.7, and absorption of 1.7% was used. Presaturated LWAs were prepared by adding 15.5% water to oven-dried, air-cooled LWAs at least 24 hours before mixing. Coarse aggregates (CA7) conforming to IDOT specifications were utilized in concrete proportioning. Tetraguard (BASF[®]) was also utilized as a shrinkage-reducing admixture. The coarse aggregate used in this study was limestone with a nominal maximum size of 19 mm. The saturated surface dry (SSD) specific gravity and absorption for the coarse aggregate were measured to be 2.69 and 2.0%, respectively. The coarse aggregate was sieved into four ranges of particle sizes—4.75 to 9.5 mm, 9.5 to 12.5 mm, 12.5 to 19 mm, and 19 to 25 mm—and then mixed with specific proportions to meet the CA7 gradation specified by IDOT.

Table 4. Chemical Composition of Raw Materials

	OPC	CSA Cement	Fly Ash
SiO ₂	20.93	7.70	59.08
Al ₂ O ₃	4.45	7.00	22.43
Fe ₂ O ₃	2.72	1.17	8.39
CaO	63.28	50.07	1.59
MgO	3.03	0.08	1.06
SO ₃	2.44	26.04	0.20
Na ₂ O	0.13	0.18	0.64
K ₂ O	0.59	0.53	2.18
LOI	1.98	2.10	2.99

Table 5. Phase Composition (%wt) of Raw Materials Obtained Using QXRD

Phase Composition	OPC	CSA Cement	Fly Ash
C ₃ S	62.2	–	–
C ₂ S	14.1	35.0	–
C ₃ A	9.9	–	–
C ₄ AF	5.4	1.5	–
Ye'elimite	–	19.4	–
Gypsum	1.4	14.7	–
Bassanite	1.6	9.4	–
Anhydrite	0.8	16.3	–
Quartz	–	–	15.8
Hematite	–	–	0.8
Periclase	1.3	0.9	–
Arcanite	0.4	–	–
Aphthitalite	0.1	–	–
Calcite	2.8	2.8	–
Mullite	–	–	21.3
Amorphous	–	–	62.2

Mixture Proportions

The work was divided into three parts.

- The first part focused on understanding the effectiveness of LWA in supplying extra water for CSA hydration. Type K concrete mixes were prepared by replacing 15% of OPC with CSA cement. The mixes with LWA were designed so that the mixture would have a “total” w/c ratio of 0.5, similar to all other mixtures. By “total,” we are considering the water retained in LWA as well as the mixing water. The mix w/c ratio (excluding the water retained in LWA) is only 0.34 for mixtures containing 20% LWA.
- The second part explored the addition of external gypsum to mitigate negative effects of class C fly ash in achieving full expansion of Type K mix.
- The third part explored a combination of SRA and Type K for shrinkage mitigation.

Tables 6, 7, and 8 show the proportions of concrete mixtures used in this study. The mix design procedure followed by IDOT was used to design the concrete mixtures. The base concrete mix was finalized using a cement factor of 610, mortar factor of 0.86, and w/cm ratio of 0.5 (including water to be contributed by LWA).

Table 6. Mixture Proportions for Concrete Specimens with Fly Ash and Gypsum

Materials		OPC	OPC_15K	OPC_15K_15FA	OPC_15K_15F A_0.5% Gypsum	OPC_15K_15F A_1% Gypsum	OPC_15K_15F A_2% Gypsum
OPC (lb/yd ³)		610	519	427	425	423	418
CSA (lb/yd ³)		0	92	91.5	91	91	90
Fly Ash (lb/yd ³)		0	0	91.5	91	91	90
Gypsum (lb/yd ³)		0	0	0	3	6	12
OD Coarse Aggregate (lb/yd ³)	19–25 mm	358	358	356	356	356	356
	12.5–19 mm	537	537	535	535	535	535
	9.5–12.5 mm	358	358	356	356	356	356
	4.75–9.5 mm	537	537	535	535	535	535
OD Sand (lb/yd ³)		1015	1015	1015	1015	1015	1015
Mixing Water (lb/yd ³)		359	359	359	359	359	359
w/c Ratio		0.5	0.5	0.5	0.5	0.5	0.5

Table 7. Mixture Proportions for Concrete Specimens with SRA

Materials		OPC_3.5SRA	OPC_7.5K_1.75SRA
OPC (lb/yd ³)		610	564
CSA (lb/yd ³)		0	46
Fly Ash (lb/yd ³)		0	0
Gypsum (lb/yd ³)		0	0
OD Coarse Aggregate (lb/yd ³)	19–25 mm	358	358
	12.5–19 mm	537	537
	9.5–12.5 mm	358	358
	4.75–9.5 mm	537	537
OD Sand (lb/yd ³)		1015	1015
Mixing Water (lb/yd ³)		346	353
SRA, Tetraguard (BASF) (lb/yd ³)		13	6
w/c Ratio		0.5	0.5

Table 8. Mixture Proportions for Concrete Specimens with LWA

Materials		OPC_20LWA	OPC_15K_20LWA
OPC (lb/yd ³)		610	518
CSA (lb/yd ³)		0	92
Fly Ash (lb/yd ³)		0	0
Gypsum (lb/yd ³)		0	0
OD Coarse Aggregate (lb/yd ³)	19–25 mm	358	358
	12.5–19 mm	537	537
	9.5–12.5 mm	358	358
	4.75–9.5 mm	537	537
OD Sand (lb/yd ³)		362	362
Mixing Water (lb/yd ³)		248	248
LWA (lb/yd ³)		599	599
Total w/c Ratio (including the water in LWA)		0.5	0.5
Mix w/c Ratio (excluding the water in LWA)		0.34	0.34

TEST METHODS

Mixing Procedure

The mixing procedure for concrete complied with ASTM C192 (ASTM 2007). The coarse and fine aggregates were initially dried in an oven and cooled before use in concrete. The amount of water to reach the saturated surface dry condition for aggregates was added separately to the mixing water. The oven-dried condition of aggregates was adopted to reduce variation due to the subjectivity of the SSD test.

Measuring Length Deformation of Concrete Samples

Three sets of samples were made, as described below:

- Set 1—Unrestrained unsealed samples: Unrestrained samples (without the steel rod) of 3 × 3 × 11.25 in. (75 × 75 × 285 mm) were prepared and cured in a sealed environment (in the mold) for 24 hours. Afterwards, the samples were demolded and cured in saturated limewater for six days before exposing them to a constant temperature ($22^{\circ}\text{C} \pm 2^{\circ}\text{C}$) and relative humidity ($50\% \pm 4\%$). Experiments were carried out in accordance with ASTM C157 (ASTM 2014).
- Set 2—Restrained unsealed samples: The samples were demolded after six hours, cured in lime-saturated water for seven days, and then exposed to 50% relative humidity to measure drying shrinkage.
- Set 3—Unrestrained sealed samples: The samples were demolded at six hours and immediately sealed to measure autogenous shrinkage.

Restrained expansion of concrete (Set 2) was monitored in accordance with ASTM C878. The 3 × 3 × 10 in. (75 × 75 × 254 mm) concrete samples were prepared in the mold shown in Figure 18. The steel rod placed at the center with attached end plates provides a restraint for the concrete. Length measurements were performed after six hours (demolding time) and 28 days. Intermediate length measurements were also taken to get more information regarding the rate of expansion. The seven-day expansion value, obtained from the restrained unsealed samples, provides useful information as it can be related to the maximum expansion experienced by a structural member in the field (ACI 223-R 2010). Length deformation was measured at a constant temperature ($22^{\circ}\text{C} \pm 2^{\circ}\text{C}$) and constant relative humidity ($50\% \pm 4\%$).

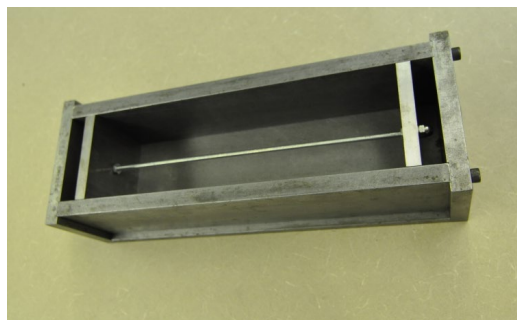


Figure 18. Photo. A typical mold for restrained expansion in accordance with ASTM C878.

EFFECTS OF COMBINING LWA AND TYPE K CEMENT

This section presents the effects of LWA on long-term deformation properties of concrete mixtures containing Type K. Long-term deformation properties of the mixture were measured and analyzed under different boundary conditions.

Figure 19 presents the unrestrained deformation results of unsealed concrete specimens. The control OPC mixture shows the highest amount of shrinkage at 168 days. The addition of Type K cement or LWA increases early-age expansion and reduces long-term shrinkage of the mixture. The mixture with only Type K cement showed a higher amount of early-age expansion. For the mixture with only Type K cement, a higher amount of expansion is expected because all water in the mix is provided to the sample as mixing water. When some of the mixing water is given to the mixture as reservoirs inside LWA, the samples showed a lower amount of early-age expansion; however, they performed better long term than the sample with only LWA. Therefore, while the Type K sample had the lowest shrinkage at 168 days, the Type K+LWA addition can be used as a good strategy to avoid excessive early-age expansion while still increasing the volume stability of the mixture.

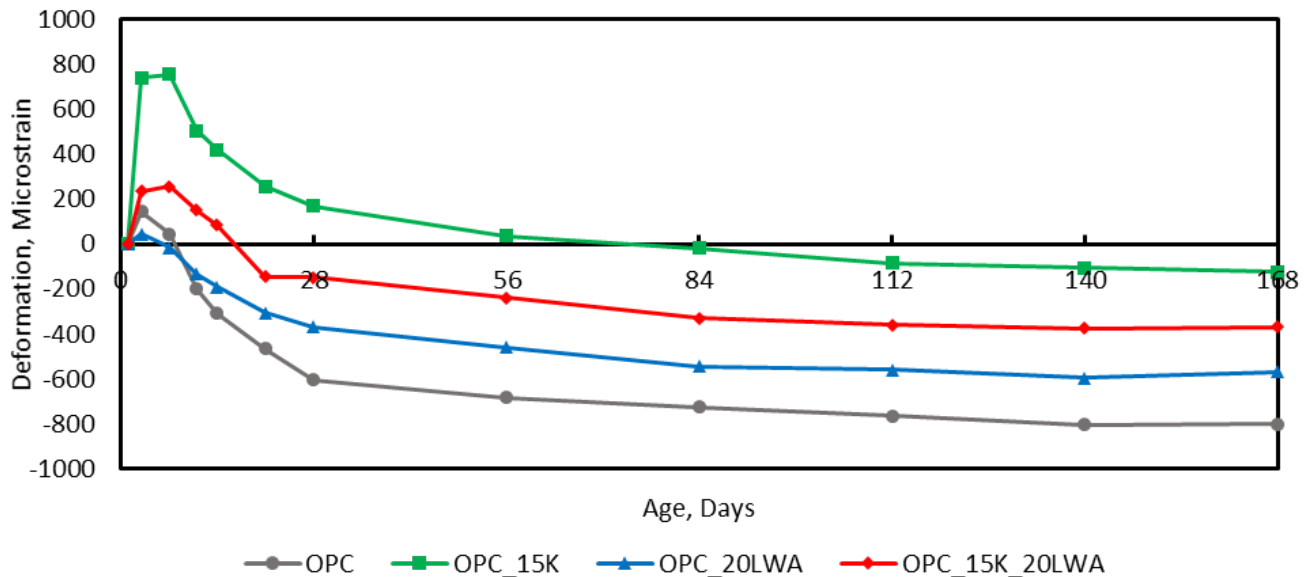


Figure 19. Graph. Effect of Type K+LWA on long-term unrestrained deformation of concrete.

Figure 20 presents the restrained deformation results of unsealed concrete specimens. Similar to unrestrained specimens, the control OPC mixture shows the highest amount of shrinkage at 168 days, and the addition of Type K cement increases early-age expansion and reduces long-term shrinkage of the mixture. Generally, mixtures with LWA show a reduced amount of drying shrinkage after being exposed to 50% relative humidity. The water reservoirs inside LWA provide internal curing for the mixture that can be used to combat the drying shrinkage of mixtures. At the end of 168 days, the measured shrinkage in the Type K and Type K+LWA samples were similar, again showing the potential benefit of combining the mitigation strategies.

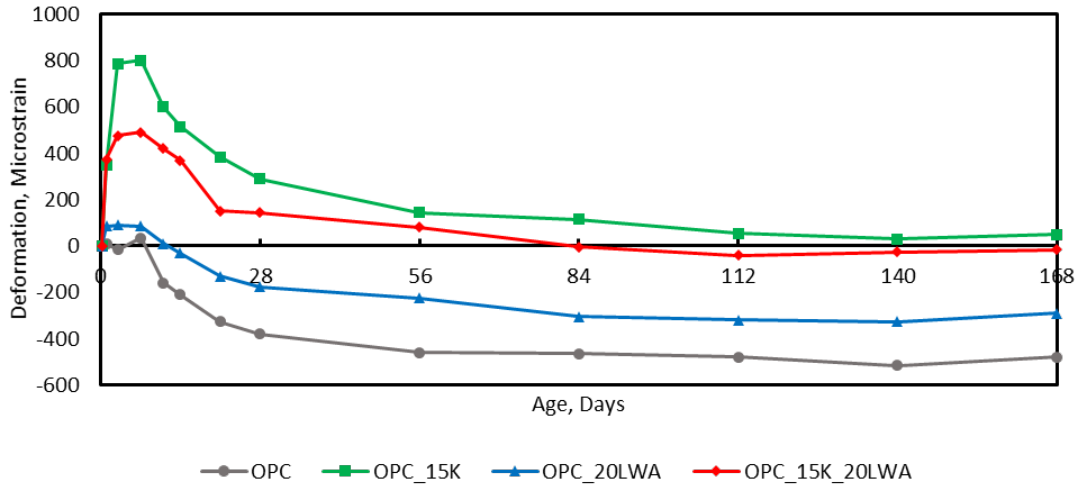


Figure 20. Graph. Effect of Type K+LWA on long-term restrained deformation of concrete.

Figure 21 presents the unrestrained deformation results of sealed concrete specimens (autogenous shrinkage). In the sealed condition, the mixtures with LWA show only minor shrinkage after the initial early-age expansion period. The water reservoirs inside LWA almost eliminate hydrogenous shrinkage completely. Therefore, the mixture with Type K cement shows a higher shrinkage at 168 days, although it showed the most early-age expansion.

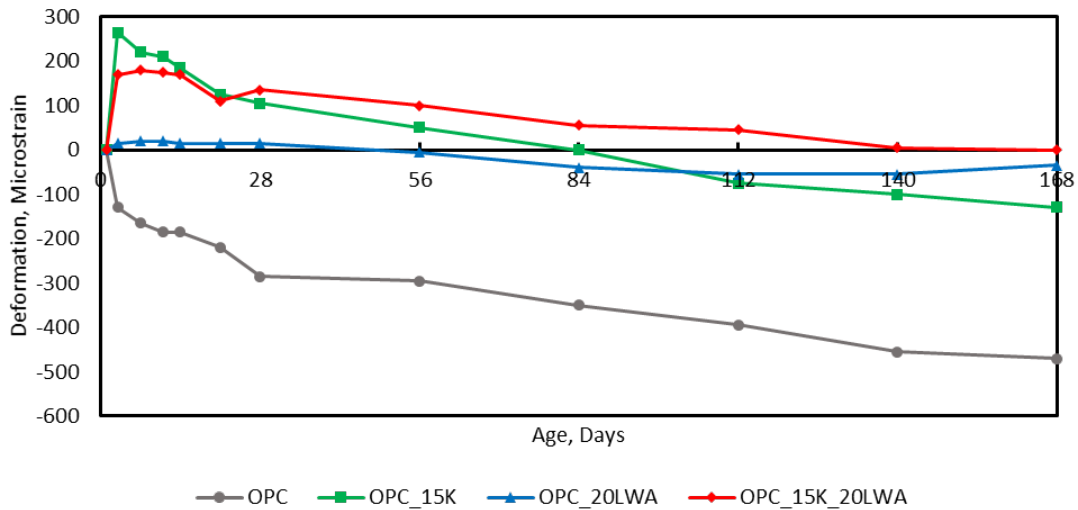


Figure 21. Graph. Effect of Type K+LWA on long-term unrestrained autogenous deformation of concrete.

VERIFYING THE NEED TO ADD EXTERNAL GYPSUM TO TYPE K CONCRETE WITH CLASS C FLY ASH

This section presents details on the effects of additional gypsum incorporation on long-term deformation properties of concrete mixtures containing Type K and class C fly ash. The second phase

of the study showed that class C fly ash can restrict the expansion of Type K mixes due to a sulfate imbalance (Ardeshirilajimi et al. 2016); however, the addition of external gypsum can mitigate negative effects in mortar samples. In this phase, concrete samples were prepared to validate the mortar data using three gypsum dosages of 0.5%, 1%, and 2% of the weight of OPC in the mixture. Long-term deformation properties of the mixture were then measured and analyzed under different boundary conditions.

Figure 22 presents the unrestrained deformation results of unsealed concrete specimens. The control OPC mixture shows the highest amount of shrinkage at 196 days, and the addition of gypsum increases early-age expansion and reduces long-term shrinkage of the mixture. Note that the mixtures with gypsum showed a continued expansion up to seven days, whereas expansion ceased at three days for the mixtures with Type K and class C fly ash. It should also be noted that the addition of 15% fly ash reduced the extent of the early expansion of the OPC_15K mixture. However, the addition of only 0.5% gypsum to OPC_15K_15FA offsets the negative effects of fly ash on early-age expansion of the OPC_15K mixture. Moreover, the excessive amount of early-age expansion for the mixture with 2% gypsum may result in microcracking of the concrete. Therefore, the amount of gypsum added should be limited to about 1%.

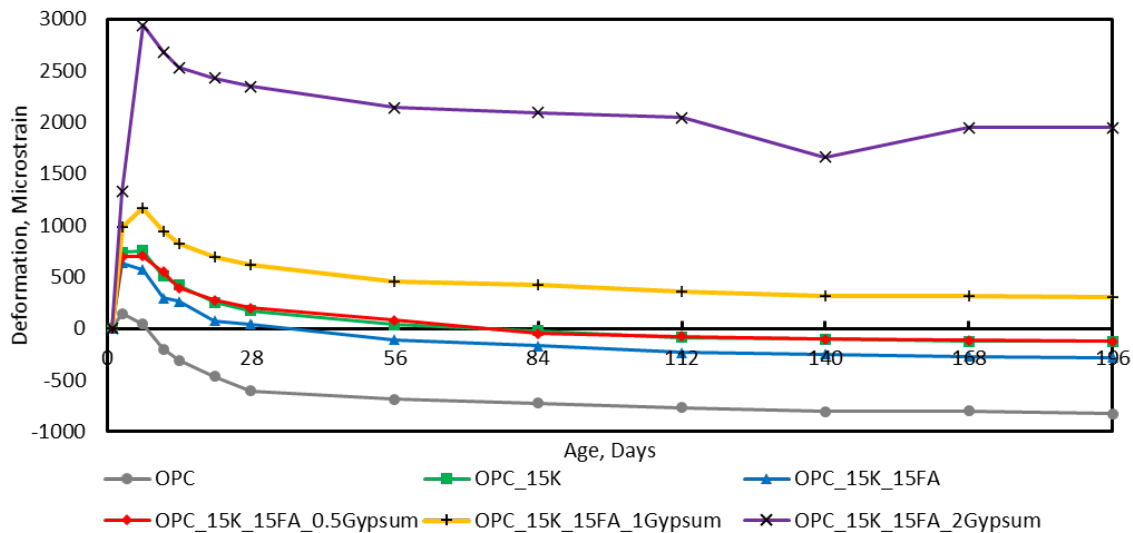


Figure 22. Graph. Effect of external gypsum addition to Type K concrete with class C fly ash: long-term unrestrained deformation of concrete.

Figure 23 presents the restrained deformation results of unsealed concrete specimens. Similar to unrestrained specimens, the control OPC mixture shows the highest shrinkage at 196 days, and the addition of gypsum increases early-age expansion and reduces long-term shrinkage of the mixture. Note that the expansion from three to seven days for most mixtures are not statistically significant; however, the mixture with 2% gypsum showed a continued expansion up to seven days. Although the addition of restraint will limit the expansion capacity of Type K cement mixtures, the built-up compressive stress will later assist the mix in offsetting tensile stress development due to autogenous shrinkage.

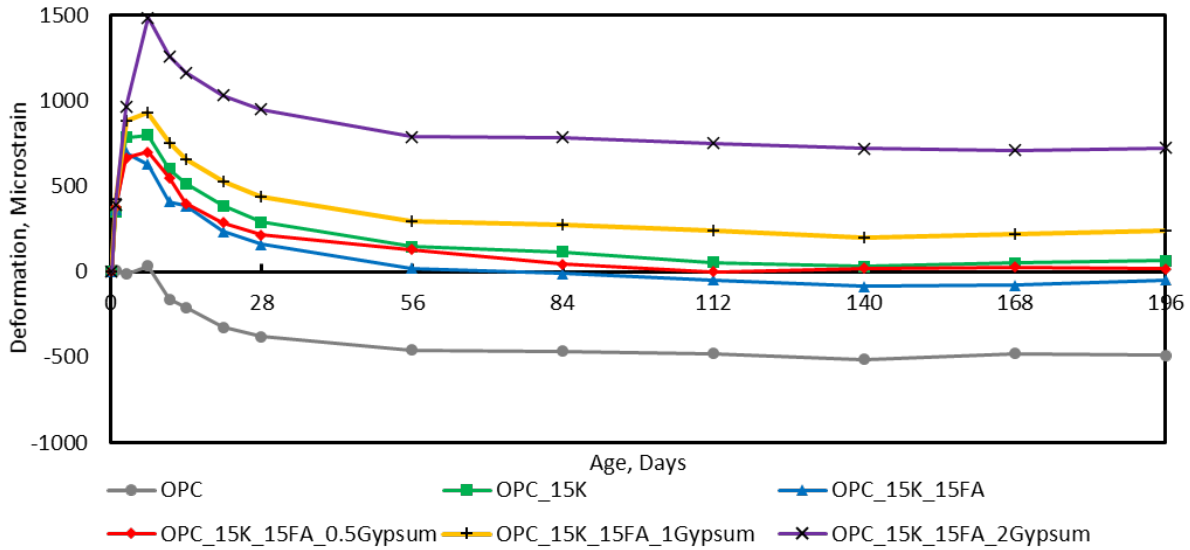


Figure 23. Graph. Effect of external gypsum addition to Type K concrete with class C fly ash: long-term restrained deformation of concrete.

Figure 24 presents the unrestrained deformation results of sealed concrete specimens (autogenous shrinkage). As expected, the control OPC mixture shows the highest shrinkage at 196 days, and the addition of gypsum increases early-age expansion and reduces long-term shrinkage of the mixture. The control mixture was the only sample that did not show early-age expansion. The rate of shrinkage beyond 28 days is greater for sealed than unsealed specimens.

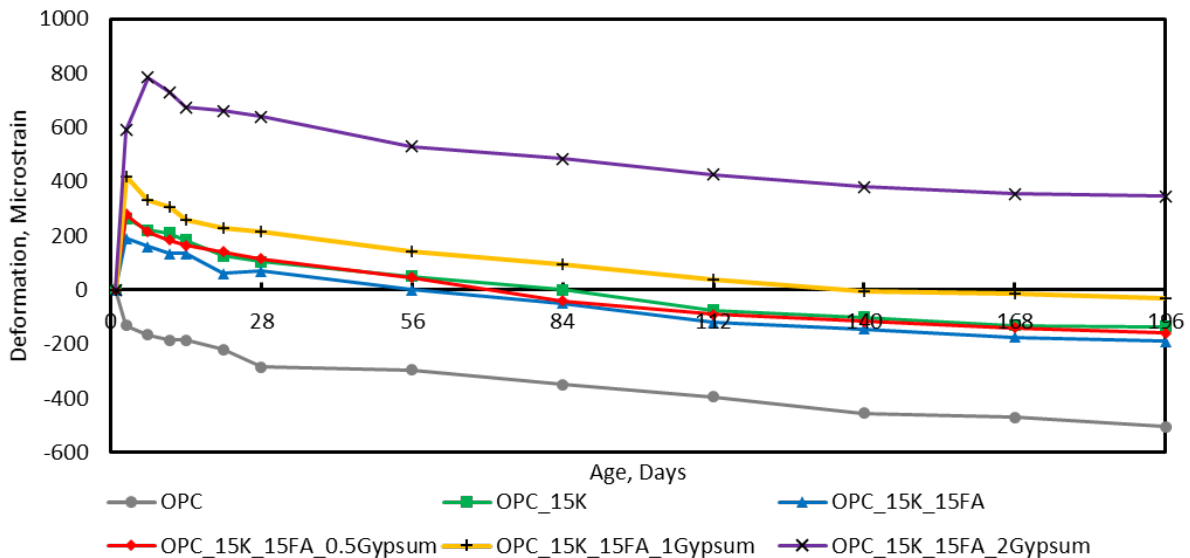


Figure 24. Graph. Effect of external gypsum addition to Type K concrete with class C fly ash: long-term autogenous deformation of concrete.

EFFECTS OF COMBINING SRA AND TYPE K FOR SHRINKAGE MITIGATION

This section presents details on the effects of combining SRA with Type K as a shrinkage-mitigation strategy. SRA was added to the mixture in two dosages, as recommended by the manufacturer. In the first mixture, SRA replaced 3.5% of the mixing water, which represents the maximum amount of SRA to be added, as noted by the manufacturer. A different mixture containing Type K cement and half the recommended dosage (1.75%) was prepared to evaluate the effects of the combination. Long-term deformation properties of the mixture were then measured and analyzed under different boundary conditions.

Figure 25 shows the unrestrained drying deformation of concrete specimens. The mixture with SRA showed increased early-age expansion and reduced drying shrinkage after the seven-day curing period. Reduced shrinkage is expected, because SRA reduces the surface tension of water inside the concrete's pores. Moreover, adding Type K cement to the mixture increased early-age expansion and reduced the shrinkage observed at 196 days. It was interesting to see that the combination strategy in the long term had similar shrinkage as the SRA only at a higher dosage. This is encouraging as the combination of Type K and SRA, both used at half the single-use dosage, can potentially reduce the negative effects of both (e.g., strength reduction, cost, ease of use) while achieving the desired shrinkage mitigation.

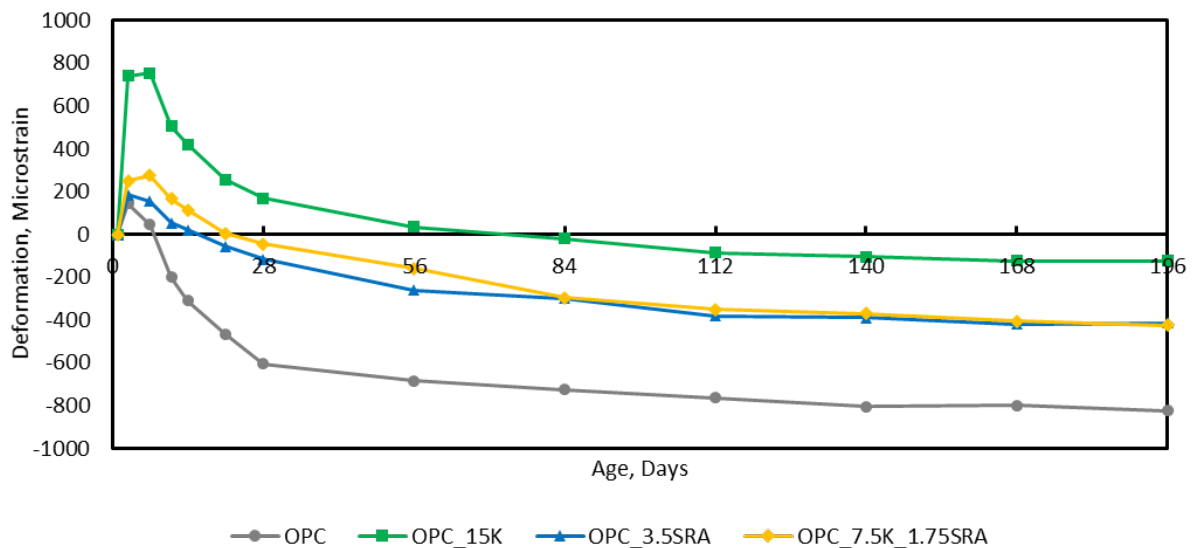


Figure 25. Graph. Combining SRA with Type K: long-term unrestrained deformation of concrete.

Figure 26 presents the restrained drying deformation of concrete specimens. As compared to Figure 29, the mixtures showed a reduction in early-age expansion during the first seven days. Again, the two mixtures with varying dosages of SRA, one with a full SRA dosage and the other with a half dosage but combined with Type K, behaved almost identically, especially after 84 days.

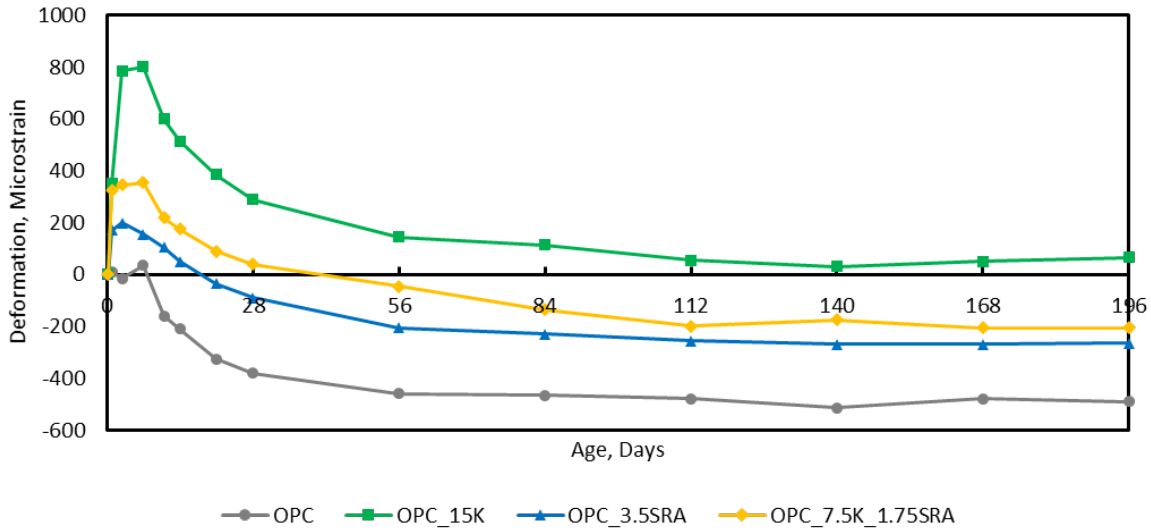


Figure 26. Graph. Combining SRA with Type K: restrained deformation of concrete.

Figure 27 presents the unrestrained (autogenous) deformation of sealed concrete specimens. Again, the addition of Type K cement to the mixture prolonged the expansion duration and increased the extent of expansion of the specimens. By comparing the slope of the lines, the mixtures with SRA showed a reduction in the amount and rate of shrinkage. At the end of 196 days, the concrete mixture with the combination strategy had the lowest shrinkage.

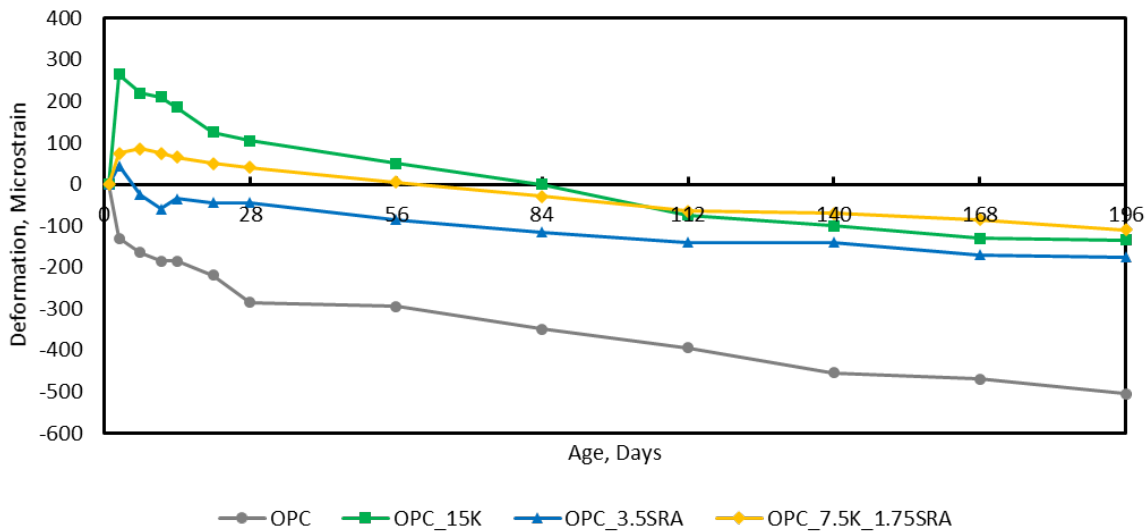


Figure 27. Graph. Combining SRA with Type K: unrestrained autogenous deformation of concrete.

SUMMARY

The results presented in this chapter confirm that combining LWA with Type K is a viable strategy for mitigating shrinkage of concrete. Presoaked LWAs can be used to supply additional water for Type K

hydration without needing to increase a mix's water-to-cement ratio. Chapter 4 highlighted the improved durability of the Type K+LWA mixture over the Type K mix. Note that the extent of early-age expansion was reduced when Type K was used in combination with LWA instead of on its own. Chapter 5 provides a further comparison of the performances of the two mixes.

The addition of class C fly ash to concrete mixtures containing Type K cement can reduce the extent of early-age expansion. This effect can be intensified with increasing the amount of class C fly ash in the mixture. Therefore, fly ash may limit the benefits of adding Type K cement to mitigate drying shrinkage and shrinkage cracking of concrete. It has been noted previously that the cause of reduced duration and magnitude of expansion in OPC–Type K–fly ash mixtures are an early depletion of gypsum. The results in this chapter showed that a small amount of gypsum added to the concrete mixture can boost early-age expansion of OPC–Type K–fly ash tertiary concrete mixtures. However, it could be difficult to achieve the targeted benefit of the gypsum addition given the complexity of homogeneous mixing of a small quantity.

Because SRA can negatively affect the strength of the concrete, this chapter also explored the possibility of using a reduced SRA dosage in combination with adding a lower dosage of Type K. The mixtures with Type K cement and SRA behaved similarly or better than the mixture with a full dosage of SRA only. This is a potential shrinkage-mitigation strategy that could be explored more carefully in the future.

CHAPTER 5: LINKING LARGE- WITH SMALL-SCALE TEST RESULTS

Concrete mixes tested in this project provide mitigation strategies for shrinkage cracking that are fundamentally different. For example, mixes incorporating Type K expand at an early age, which counteracts the shrinkage that develops later. In contrast, SRA incorporation directly reduces the shrinkage of concrete. Therefore, it is difficult to compare their effectiveness directly by looking at only shrinkage or expansion measurements. This shows the need to develop a standardized test method to compare performances of various mixes. The dual ring test is one such test that could be explored in the future. Within the scope of this project, we relied on extensive data analysis on both large- and small-scale testing to ultimately rank mixes based on their performance in mitigating cracking due to shrinkage.

At the University of Illinois at Urbana-Champaign and University of Delaware, a strain measurement of plain concrete without reinforcement was performed at the small scale using $3 \times 3 \times 10$ in. ($75 \times 75 \times 254$ mm) samples. In this case, concrete samples were free to deform. However, the structural testing was performed at Saint Louis University, where a model concrete deck was tested and concrete was internally and externally restrained using rebars, end supports, and connection to girders (Rahman et al. 2020). Measured strains from both tests were vastly different. Therefore, this chapter presents extensive data analysis to explore the relationship between both tests using four to five concrete mixes with the most promising shrinkage-mitigation strategies.

EFFECTS OF RESTRAINT IN SMALL-SCALE TESTING

Before comparing strains measured in small-scale testing with the large scale, the effect of using restraint is explored in the small scale. As per ASTM C878, the expansion of expansive concrete is monitored using $3 \times 3 \times 10$ in. ($75 \times 75 \times 254$ mm) samples, where a steel rod is placed at the center with attached end plates to provide restraint. The same test setup was used for all other mixes to understand the effect of restraint at the small scale. Five mixes were selected for this analysis: control, LWA, Type K, Type K+LWA, and SRA.

Figure 28 presents the restrained-to-unrestrained shrinkage ratio for 168 days, where the restraint reduced measured shrinkage. For all samples, restraint shrinkage varied between 60% to 90% of the free (unrestrained) shrinkage. There is some variation between the mixes; however, for a same mix, the ratio did not change much over the 168 day period.

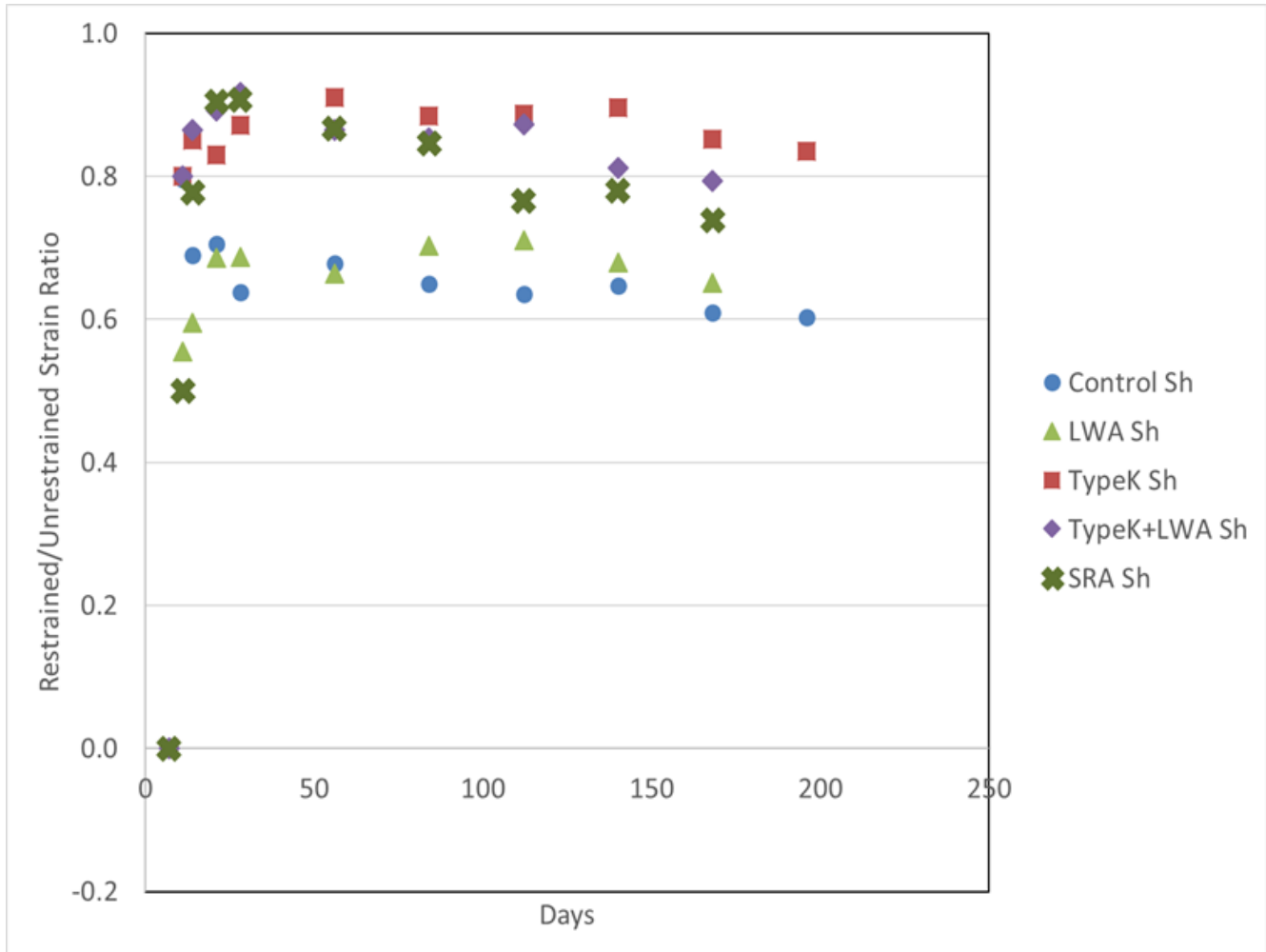
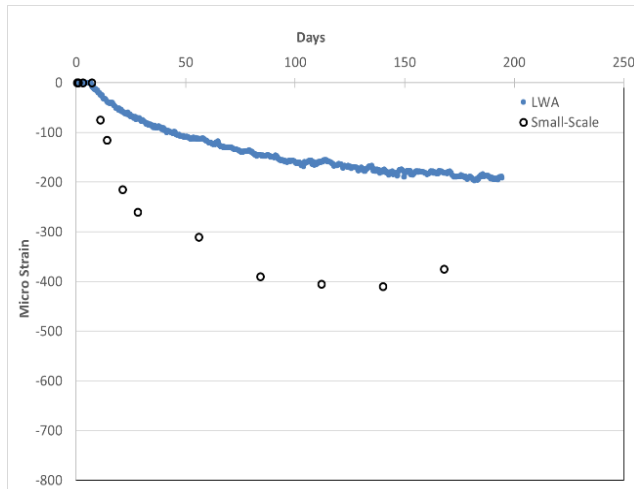


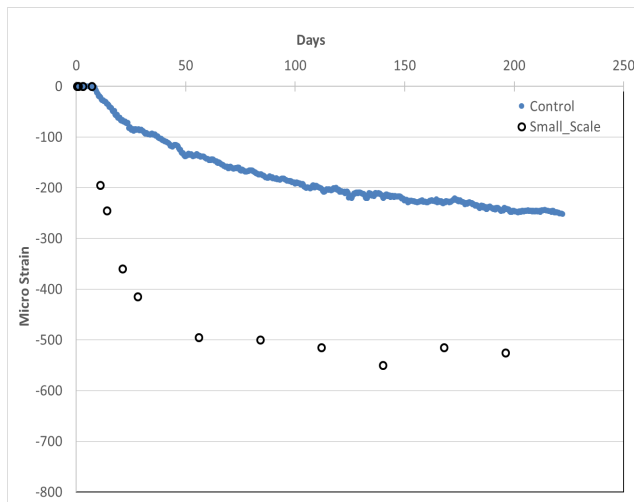
Figure 28. Graph. Restrained-to-unrestrained shrinkage ratio.

COMPARING LARGE- TO SMALL-SCALE STRAIN MEASUREMENTS

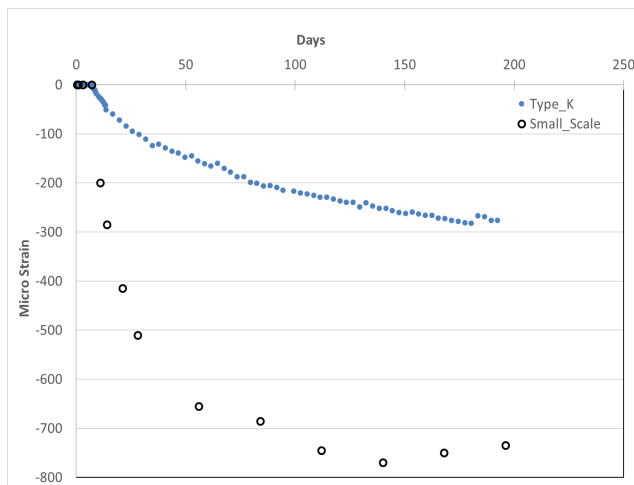
This section compares the strains measured in small-scale testing with the large scale using four key mixes: control, LWA, Type K, and Type K+LWA. Figure 29 compares the shrinkage measured at the small scale (restrained shrinkage with the steel rob and end plates) and large scale for all mixes for about six months. Because water curing was used for both the small-scale samples and large-scale models, expansion was observed during the first seven days and shrinkage was only observed once the water curing was stopped and small-scale samples were exposed to 50% relative humidity whereas large-scale models were exposed to the lab condition. Based on the higher level of restraints and milder exposure, the large-scale models are expected to exhibit lower shrinkage, which is evident from Figure 29. Another difference is that the small-scale samples achieved their respective maximum shrinkage sooner than the large-scale models. Shrinkage in the small-scale samples leveled off around three months, whereas large-scale models continued to experience increased shrinkage. Increased degree of restraint in the large-scale model decks seemed to have not only reduced the ultimate shrinkage measured, but also reduced the rate of shrinkage and extended the duration during which shrinkage occurred.



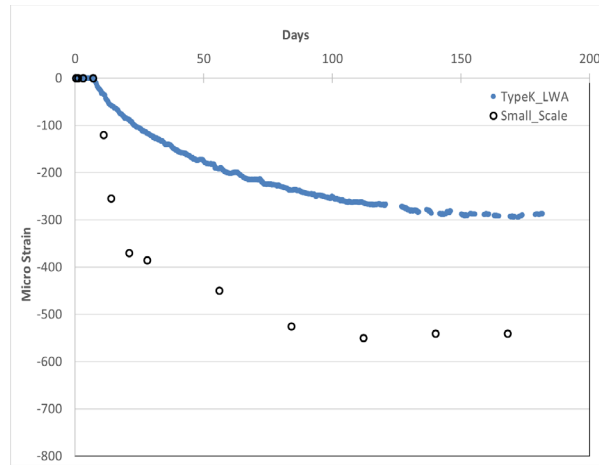
(A) LWA



(B) Control

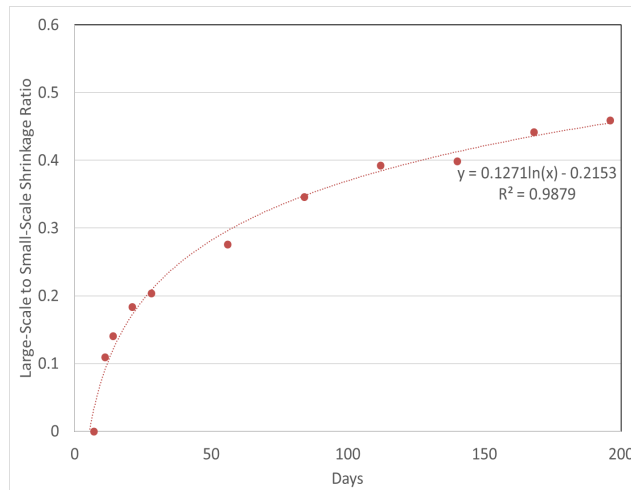


(C) Type K

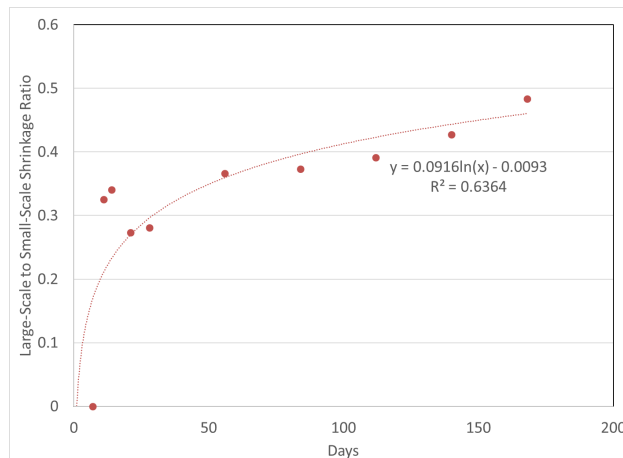


(D) Type K+LWA

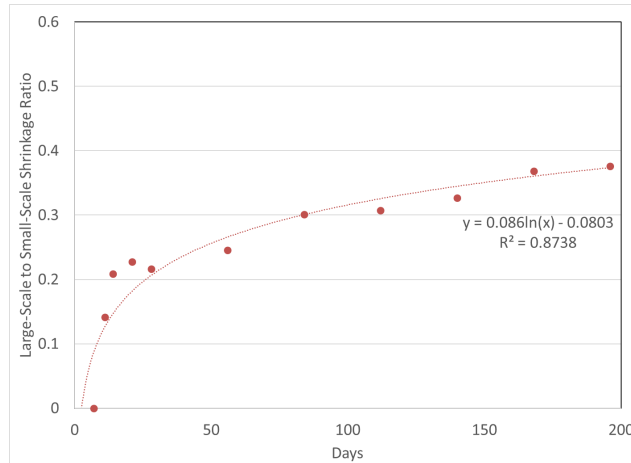
Figure 29. Graph. Shrinkage measured in small-scale testing and large-scale model deck.



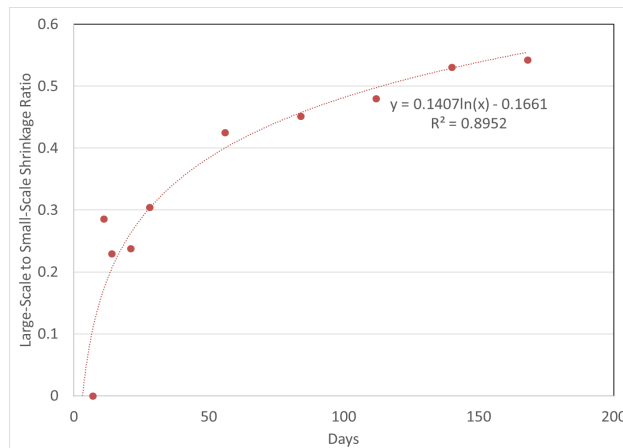
(A) Control



(B) LWA



(C) Type K



(D) Type K+LWA

Figure 30. Graph. Ratio of shrinkage measured in small-scale testing and large-scale model deck.

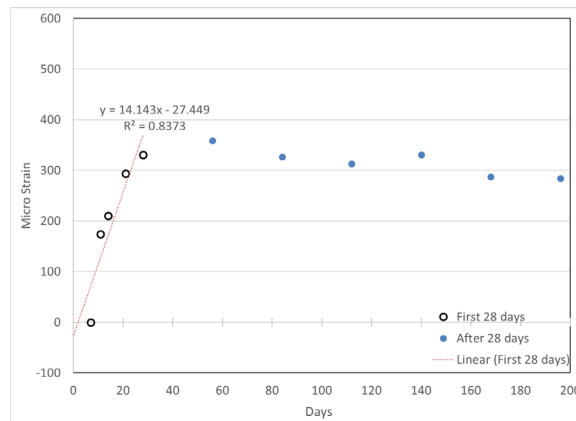
Given the large-scale models showed substantially less shrinkage for all mixes, the nature of this difference was analyzed further. The ratio of shrinkage measured in micro strain for large-scale models to the small-scale samples for control, LWA, Type K, and Type K + LWA mixes were calculated and plotted in Figure 30. Important observations based on the figure are as follows:

- The ratio increases at a high rate early on, allowing for logarithmic curve fitting. The difference between the shrinkage measured in small-scale samples and the large-scale model is largest and changing rapidly early on. A similar observation can also be noted from Figure 29.
- At the end of six months, for all samples except Type K, the ratio of large- to small-scale shrinkage is consistent and varies within 0.5 ± 0.05 . This means that the increased degree of restraint in the large-scale model stayed consistent between different models and even between the different phases of this project. It also suggests that the measurements from small-scale samples can capture the behavior of the large-scale model well, despite differences.

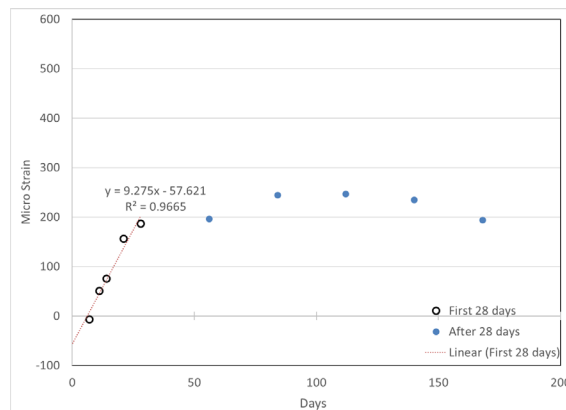
- The Type K mix showed significantly smaller shrinkage than other mixes, with a shrinkage ratio of less than 0.4. This indicates two possibilities: either the mixes used in the small scale and the large scale were significantly different in spite of the coordination between the two research groups, or the model deck for the Type K mix has unusually higher restraint towards shrinkage.

Because the difference between the shrinkage measured in small-scale samples and the large scale-scale model is the largest and changing rapidly early on, we employed another method to visualize the difference further. We plotted the difference in shrinkage (measured in micro strain) for all four mixes in Figure 31, from which we can make the following observations:

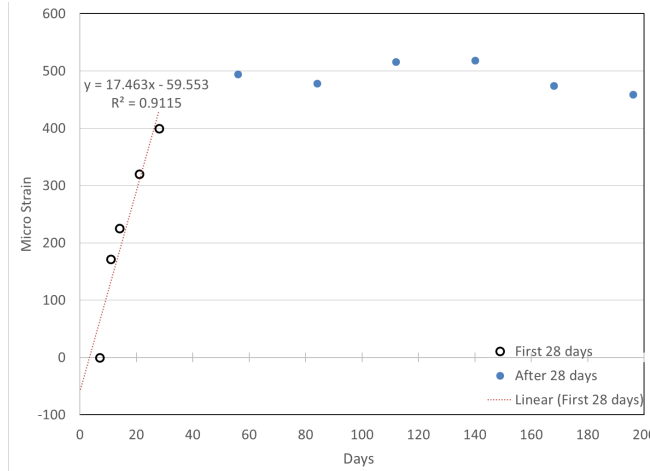
- The difference between the two shrinkage measurements increases rapidly in a linear fashion within the first 28 days of drying exposure.
- After the first 28 days, the difference between the two shrinkages is constant. At this level, the difference in shrinkage for all samples except Type K varies within 300 ± 50 micro strain. For Type K, this difference was much higher at 500 micro strain, showing again that the large-scale model had unusually lower shrinkage for the Type K mix. The LWA mix showed the lowest difference in shrinkage.



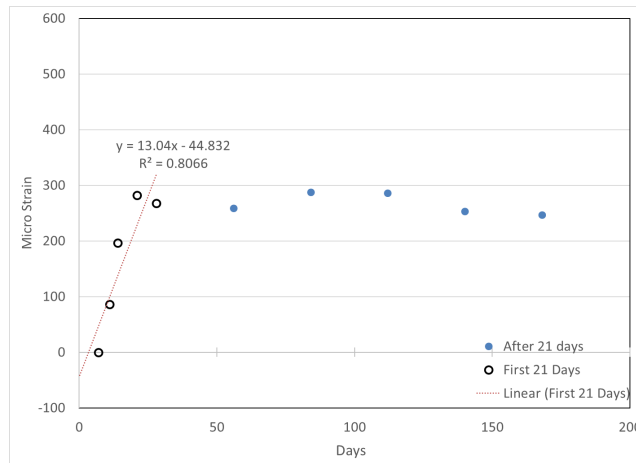
(A) Control



(B) LWA



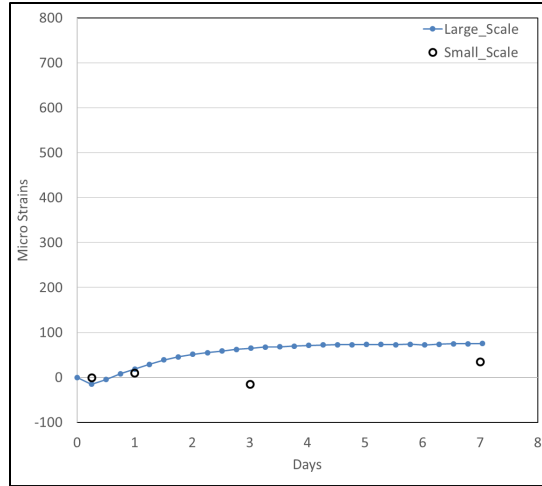
(C) Type K



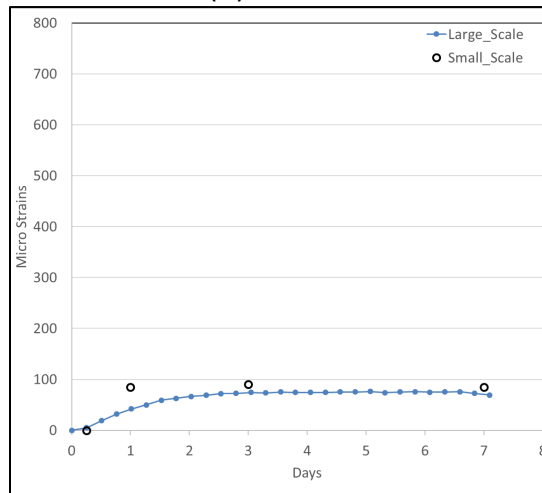
(D) Type K+LWA

Figure 31. Graph. Difference in shrinkage measured in small-scale testing and large-scale model deck.

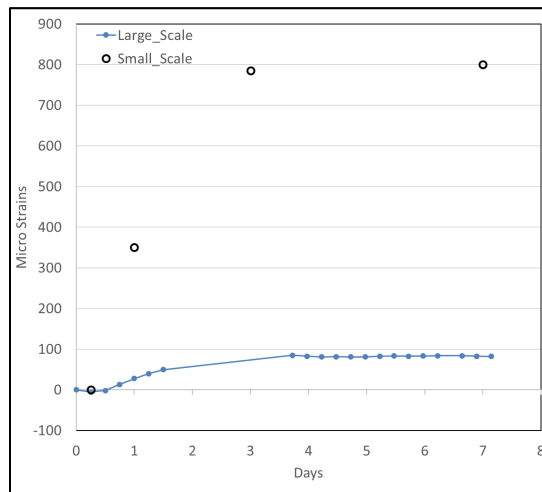
Figure 32 compares the expansion that occurs during the first seven days for all mixes. Both the control and LWA mixes showed little expansion compared to the other two mixes with Type K. The large-scale model for the control mix showed higher expansion than even the small-scale samples in some cases. For the LWA mix, the expansion in both tests seemed to be comparable. For both Type K mixes, small-scale samples showed significantly higher expansion compared to the large-scale model. To understand the difference between the measured expansion in both cases, further analysis has been performed and presented in Figures 32 through 34.



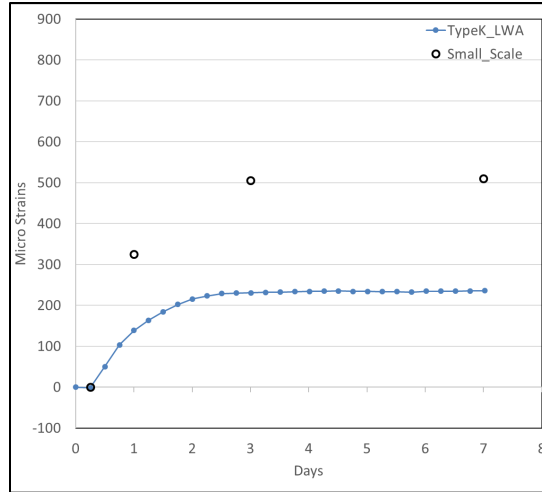
(A) Control



(B) LWA

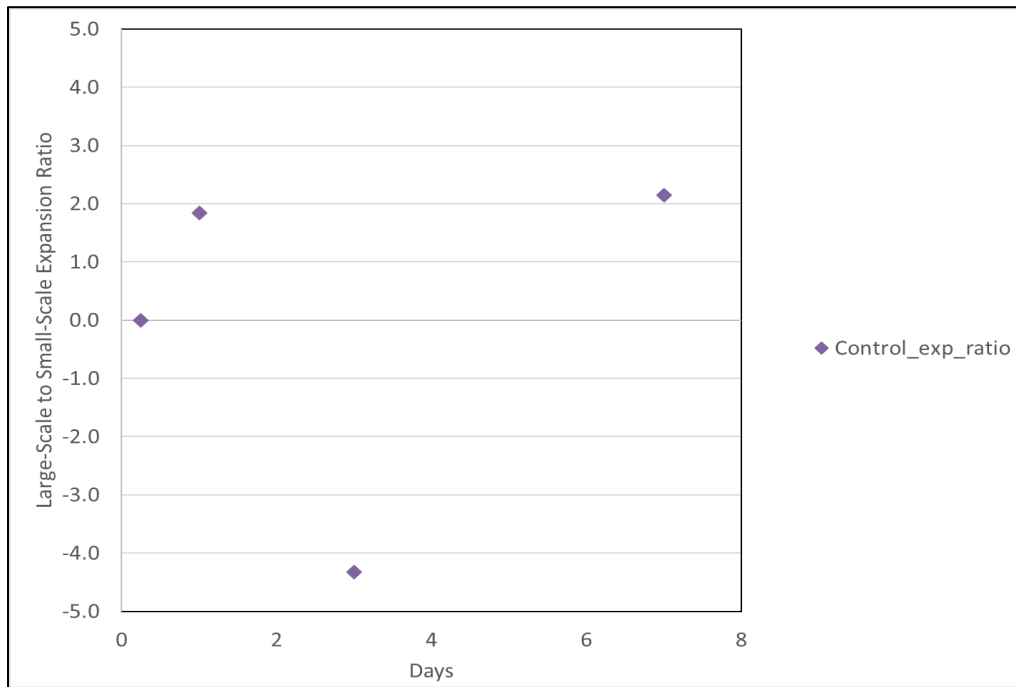


(C) Type K

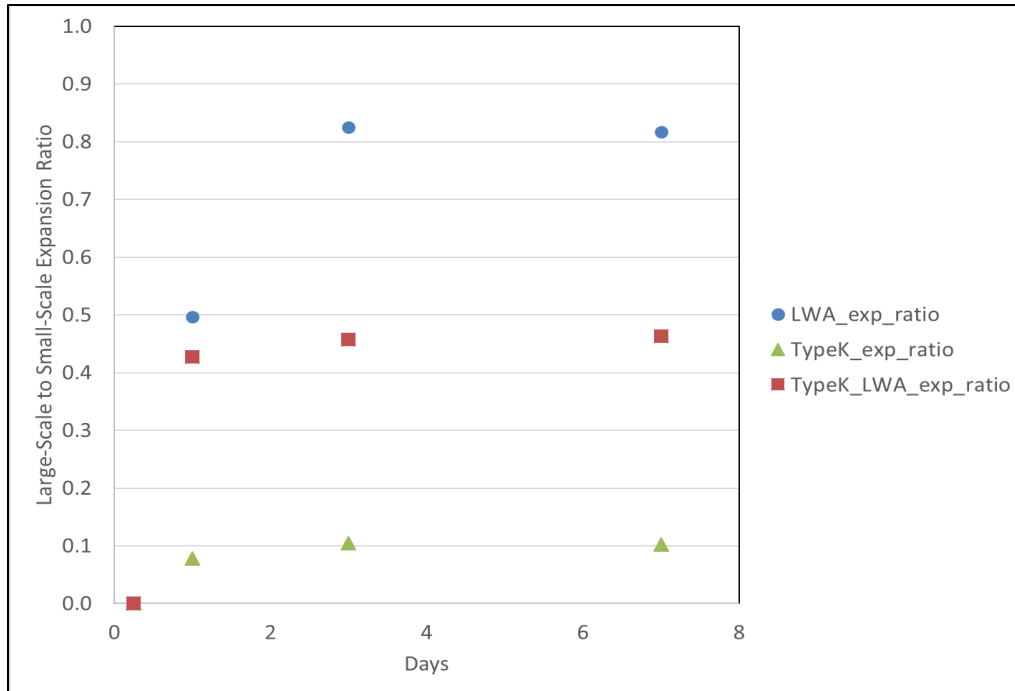


(D) Type K+LWA

Figure 32. Graph. Difference in expansion measured in small-scale testing and large-scale model deck.



(A) Control



(B) LWA, Type K, and Type K+LWA

Figure 33. Graph. Ratio of expansion measured in small-scale testing and large-scale model deck.

Similar to the analysis performed for shrinkage data, we first calculated the ratio of expansion measured during the first seven days of water curing for large-scale models to the small-scale samples for control, LWA, Type K and Type K + LWA mixes and plotted it in Figure 33. Important observations based on the figure are as follows:

- The small-scale samples experienced very little expansion for the control mix, and the expansion ratio varied randomly over a wide range.
- The expansion ratio increased significantly within the first three days and then leveled off for the other three samples.
- Unlike shrinkage, the magnitude of the stable expansion ratio after three days varied significantly between the mixes.
- The large-scale model with LWA showed 80% of the expansion measure in the small-scale sample (stable expansion ratio of 0.8), whereas the large-scale Type K model showed only 10% expansion of the small-scale samples (stable expansion ratio of 0.1). The Type K+LWA mix has a stable expansion ratio value in the middle, around 0.45, the only case where the stable expansion ratio value is similar to the final shrinkage ratio plotted in Figure 33.

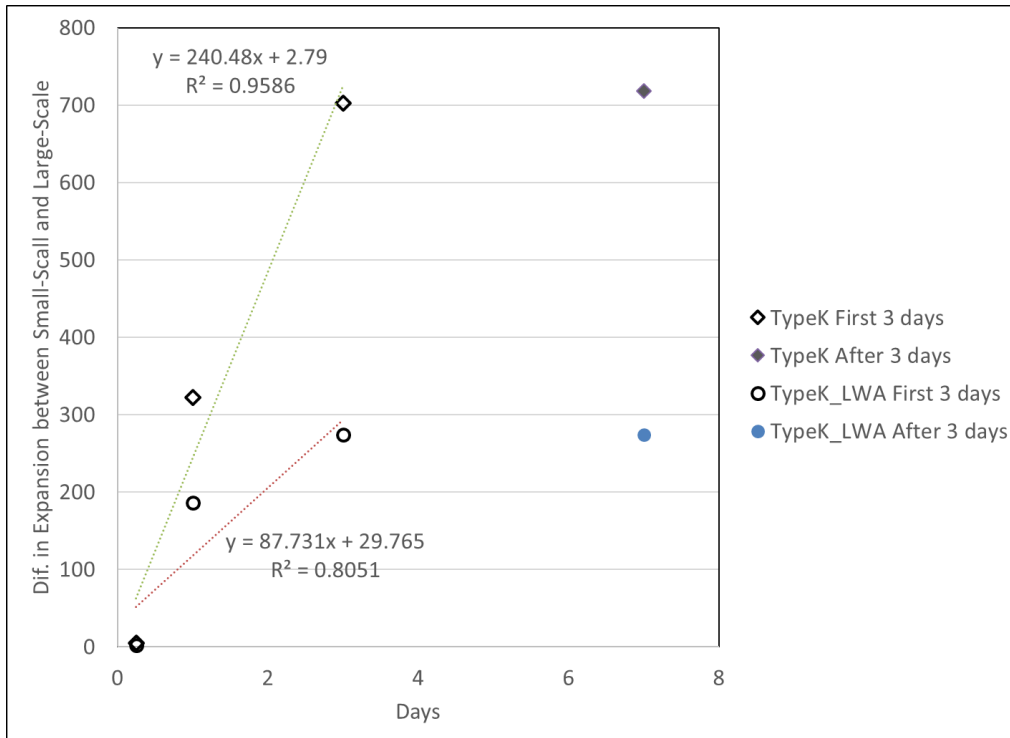


Figure 34. Graph. Difference in expansion measured in small-scale testing and large-scale model deck.

The comparison between the calculated expansion ratio and shrinkage ratio brings up other important points. Assuming the small-scale samples had little restraint against expansion and shrinkage, it seems the large-scale model did not offer similar restraint against expansion and shrinkage. This is most likely related to the source of the restraint. C channels used along the edge of the model deck are expected to be effective in restraining expansion, but not shrinkage. Reinforcement also offers internal restraint; however, its effectiveness varies with time, as it depends on the development of bond. It is also interesting that the expansion ratio leveled off after three days but the shrinkage ratio for large- to small-scale did not. However, the shrinkage ratio did level off again for small-scale restrained to unrestrained. This indicates that the large-scale models did not achieve their full shrinkage potential even after six months. The shrinkage in the small-scale samples leveled off after three months, whereas even at the end of six months, large-scale samples had a mild slope to the shrinkage data, showing a continued trend of increasing shrinkage. This highlights the long-term nature of shrinkage deformation where restraints are present that prolong the duration of shrinkage.

Figure 34 compares the difference between the expansion measured from small-scale samples to the large-scale models only for the two cases with Type K. Similar to shrinkage, the difference increased linearly early on, for the first three days in this case, and then leveled off. The difference in the slope of the linear fit during the first three days and the stable value of the difference in expansion after the first three days both show that the large-scale Type K model had unexpectedly lower expansion than the Type K + LWA mixture.

PERFORMANCE COMPARISON OF MIXES BASED ON TENSILE STRESS DEVELOPED AND CRACKING POTENTIAL

The large-scale tests were performed as a steppingstone between the small-scale material tests and a real-world bridge deck. In the model deck, the external restraint was provided by four C channels placed along the edges of the concrete deck and bolted to the rebars, and the internal restraint was provided by the frictional bond between the rebars and concrete as well as shear studs attached to the steel girders. In contrast, shrinkage measured in the small-scale test was either unrestrained or restrained using a small rebar inside concrete and two end plates. The unrestrained small-scale samples provide the total shrinkage potential of any mix. Part of this total shrinkage is measured in the large-scale model deck and the rest disappears due to increased internal and external restraint. This missing shrinkage strain ultimately ends up developing tensile stress in the concrete and can lead to cracking if the developed tensile stress at any point exceeds the tensile strength of the concrete.

Table 9 and Table 10 show sample stress analysis for Type K and Type K+LWA mixes, respectively. Compressive strength of the concrete used to cast the model deck was measured by the Saint Louis University research team at 7, 14, and 28 days and was used to predict strength at 168 days (Rahman et al. 2020). Tensile strength and modulus of elasticity was calculated based on the ACI formula. The stress developed is calculated based on the missing strain in the large scale compared to the small-scale unrestrained sample, and modulus of elasticity is calculated given the measured compressive strength. As demonstrated from the values of the stresses developed, the Type K model deck concrete was actually under compression (because tensile stress was assumed to be negative) during all ages tested. Therefore, the cracking potential of the concrete was none (negative).

Table 9. Stress Analysis for Type K

Days	Measured or Predicted Comp. Strength (psi)	Predicted Tensile Strength	Modulus of Elasticity (psi)	Stress Developed (Tension -ve)	Cracking Potention
7	3,030	-356	3,137,590	2,196	-7.17
14	3,690	-406	3,462,486	1,469	-4.62
28	4,340	-452	3,755,085	811	-2.79
168	5,425	-525	4,198,312	386	-1.74

Table 10. Stress Analysis for Type K+LWA Mix

Days	Measured or Predicted Comp. Strength (psi)	Predicted Tensile Strength (psi)	Modulus of Elasticity (psi)	Stress Developed (Tension -ve)	Cracking Potention
7	4,259	-447	3,719,878	626	-2.40
14	5,205	-511	4,112,304	-291	-0.43
28	5,857	-552	4,362,269	-596	0.08
168	7,321	-641	4,877,165	-1075	0.68

For the Type K+LWA deck, the stress developed was compressive only at seven days and became tensile after that. At 14 days, the developed tensile stress was significantly lower than the tensile strength of the concrete at that age; however, at 28 days the stress became almost equal to the

strength. At 168 days, the tensile stress developed significantly exceeded the tensile strength of concrete at that age.

Based on the above analysis, the Type K+LWA deck should have cracked after 28 days; however, no crack formation was observed. Therefore, it is important to understand that the above analysis is conservative. One of the primary sources of error is concrete creep, which is particularly high during early age. The modulus of elasticity of concrete under compression and tension could also be very different. Furthermore, the ACI equations to calculate modulus of elasticity and tensile strength may not be equally applicable for different mixes, as we deviated from a control mixture. Because of these reasons, it would be better to compare performance experimentally in the future using a dual ring test.

Nonetheless, effort has been made to rank the performance of the five most promising mixes for their effectiveness in shrinkage crack mitigation based on the cracking potential calculated at various ages. Table 11 and Table 12 show the ranking at 28 days and 168 days, respectively. In all ages, the Type K mix showed the best performance, and the control mix showed the worst performance. The Type K+LWA and SRA mixes showed similar performance up to 28 days, after which the Type K+LWA mix performed better. The LWA mix consistently performed better than the control mix; however, performance improved when used in combination with Type K.

Table 11. Performance Ranking of Mixes at 28 days

	Rank	Mix	Cracking Potential at 28 days
Best	1	Type K	-2.79
	2	SRA	-0.09
	3	Type K + LWA	0.08
	4	LWA	1.63
Worst	5	Control	3.83

Table 12. Performance Ranking of Mixes at 168 days

	Rank	Mix	Cracking Potential at 168 days
Best	1	Type K	-1.74
	2	SRA	0.68
	3	Type K + LWA	1.88
	4	LWA	2.20
Worst	6	Control	4.07

SUMMARY

In-depth data analysis showed that for all samples except Type K the ratio of large- to small-scale shrinkage is consistent and varies within a small range. In spite of the big difference in the measured strain between small- and large-scale testing, the small-scale data only deferred by a scaling factor and otherwise captured the behavior of the large-scale model well. The increased degree of restraint in the large-scale model stayed consistent between different models. Stress analysis was performed based on the free shrinkage potential of each mix as measured in the small scale and the missing

strain in the model deck due to restraint. Though it is not perfect because it does not consider early-age creep of concrete, the analysis helps to rank the performance of shrinkage-mitigation strategies that are based on different fundamental mechanisms. Based on the analysis, the Type K mix is ranked as the best and the control mix is ranked as the worst performer at all ages. Type K+LWA and SRA mixes are ranked either second or third, depending on the age. The LWA mix is ranked as the least-effective shrinkage-mitigation strategy; however, it consistently performed better than the control mix.

CHAPTER 6: CONCLUSIONS

The main conclusions for this study are as follows:

- No significant difference in admixture interaction between conventional and Type K concrete was observed. A mid-range water reducer (MasterPolyheed 1020) worked better than a high-range water reducer in both the control and Type K concrete mixes. This does not, however, eliminate the possibility of using a high-range water reducer effectively in the future, because dosage optimization was outside the scope of this study.
- Use of presoaked LWAs made an impact in reducing water absorption of Type K concrete. The positive effect can be attributed towards the internal curing mechanism of presoaked LWAs. Use of presoaked LWAs offers a viable method to provide extra water for Type K hydration and, hence, the use of Type K as a shrinkage-mitigation strategy without the need for increasing the water-to-cement ratio of concrete.
- Type K should be used with caution as a shrinkage-mitigation strategy if class C fly ash is also being used in the concrete, as the latter can reduce the extent of early-age expansion. This effect can be intensified by increasing the amount of class C fly ash in the mixture. A small addition of gypsum to the concrete mixture can counteract the negative impact of class C fly ash if proper homogeneous mixing of gypsum is achieved in spite of the small quantity needed.
- Based on the limited work within the scope of this project, SRA in combination with Type K can be an effective shrinkage-mitigation strategy and could be explored more carefully in the future. It combines the benefits of two methods of combating shrinkage while keeping their individual side effects within limit because of their relatively smaller dosages.
- In spite of the big differences in the measured strain between small- and large-scale testing, small-scale data only deferred by a scaling factor and otherwise captured the behavior of the large-scale model well. The increased degree of restraint in the large-scale model stayed consistent between different models.
- Though it does not consider early-age creep of concrete, stress analysis still can be helpful in ranking the performance of shrinkage-mitigation strategies that are based on different fundamental mechanisms.
- Based on the stress analysis, the Type K mix is ranked as the best, and the control mix is ranked as the worst performer at all ages. Type K+LWA and SRA mixes are ranked either second or third, depending on the age. The LWA mix is ranked as the least-effective shrinkage-mitigation strategy; however, it consistently performed better than the control mix.

REFERENCES

- ACI Committee 231. 2010. *Report on Early-Age Cracking: Causes, Measurement, and Mitigation*. Farmington Hills, MI: American Concrete Institute.
- American Society of Testing Materials (ASTM). 1997. *ASTM C642-13. Standard Test Method for Density, Absorption, and Voids in Hardened Concrete ASTM C-642*. West Conshohocken, PA: ASTM International.
- . 2001. *ASTM C 685/C 685M-01. Standard Specification for Concrete Made by Volumetric Batching and Continuous Mixing*. West Conshohocken, PA: ASTM International.
- . 2003. *ASTM C878/C878M. Standard Test Method for Restrained Expansion of Shrinkage-Compensation Concrete*. West Conshohocken, PA: ASTM International.
- . 2004. *ASTM C128. Standard Test Method for Density, Relative Density (Specific Gravity), and Absorption of Fine Aggregate*. West Conshohocken, PA: ASTM International.
- . 2007. *ASTM 192 Standard Practice for Making and Curing Concrete Test Specimens in the Laboratory*. West Conshohocken, PA: ASTM International.
- . 2010. *Standard Test Method for Air Content of Freshly Mixed Concrete by the Pressure Method*. West Conshohocken, PA: ASTM International.
- . 2013. *ASTM C1585-13. Standard Test Method for Measurement of Rate of Absorption of Water by Hydraulic Cement Concretes*. West Conshohocken, PA: ASTM International.
- . 2014. *ASTM Standard C157—Standard Test Method for Determination of One-Point, Bulk Water Sorption of Dried Concrete*. West Conshohocken, PA: ASTM International.
- . 2015. *ASTM C143/C143M. Standard Test Method for Slump of Hydraulic-Cement Concrete*. West Conshohocken, PA: ASTM International.
- Ardeshirilajimi, Ardavan, Di Wu, Piyush Chaunsali, Paramita Mondal, Ying Tung Chen, Mohammad Mahfuzur Rahman, Ahmed Ibrahim, Will Lindquist, and Riyadh Hindi. 2016. *Bridge Decks: Mitigation of Cracking and Increased Durability*. Rantoul, IL: Illinois Center for Transportation.
- Bentz, Dale P., and W. Jason Weiss. 2011. *Internal Curing: A 2010 State-of-the-Art Review*. Washington, DC: US Department of Commerce, National Institute of Standards and Technology.
- Chaunsali, Piyush, Seungmin Li, Paramita Mondal, Douglas Foutch, Doug Richardson, Ying Tung, and Riyadh Hindi. 2013. *Bridge Decks: Mitigation of Cracking and Increased Durability*. Rantoul, IL: Illinois Center for Transportation.
- Collepari, Mario. 2005. "Chemical Admixtures Today." *Proceedings of the Second International Symposium on Concrete Technology*, Hyderabad, India, February 27–March 3.
- Day, Ken W., James Aldred, and Barry Hudson. 2013. *Concrete Mix Design, Quality Control and Specification*. London: Taylor & Francis Group.
- Du, Lianxiang, and Kevin J. Folliard. 2005. "Mechanisms of Air Entrainment in Concrete." *Cement and Concrete Research* 35 (8): 1463–71. <https://doi.org/10.1016/j.cemconres.2004.07.026>.
- Fu, Yan, Ping Gu, Ping Xie, and J. J. Beaudoin. 1995. "Effect of Chemical Admixtures on the Expansion

- of Shrinkage-Compensating Cement Containing a Pre-Hydrated High Alumina Cement-Based Expansive Additive." *Cement and Concrete Research* 25 (1): 29–38. [https://doi.org/10.1016/0008-8846\(94\)00109-C](https://doi.org/10.1016/0008-8846(94)00109-C).
- Goual, M. S., F. de Barquin, M. L. Benmalek, A. Bali, and M. Quéneudec. 2000. "Estimation of the Capillary Transport Coefficient of Clayey Aerated Concrete Using a Gravimetric Technique." *Cement and Concrete Research* 30 (10): 1559–63. [https://doi.org/10.1016/S0008-8846\(00\)00379-3](https://doi.org/10.1016/S0008-8846(00)00379-3).
- Hosoda, A. 2007. "Self Healing of Crack and Water Permeability of Expansive Concrete." *First International Conference on Self Healing Materials*, Noordwijk, The Netherlands, April 18–20.
- Huang, Guangping, Deepak Pudasainee, Rajender Gupta, and Wei Victor Liu. 2019. "Hydration Reaction and Strength Development of Calcium Sulfoaluminate Cement-Based Mortar Cured at Cold Temperatures." *Construction and Building Materials* 224: 493–503. <https://doi.org/10.1016/j.conbuildmat.2019.07.085>.
- Martys, Nicos S., and Chiara F. Ferraris. 1997. "Capillary Transport in Mortars and Concrete." *Cement and Concrete Research* 27 (5): 747–60.
- Mehta, P. K. 1999. "Concrete Technology for Sustainable Development: An Overview of Essential Principles." In *Vancouver CANMET/ACI International Symposium on Concrete Technology for Sustainable Development*.
- Neithalath, Narayanan. 2006. "Analysis of Moisture Transport in Mortars and Concrete Using Sorption-Diffusion Approach." *ACI Materials Journal* 103 (3): 209–17.
- Neville, Adam. 2001. "Consideration of Durability of Concrete Structures: Past, Present, and Future." *Materials and Structures* 34 (2): 114–18. <https://doi.org/10.1007/BF02481560>.
- Parrott, L. J. 1994. "Moisture Conditioning and Transport Properties of Concrete Test Specimens." *Materials and Structures* 27 (8): 460–68.
- Powers, T C. 1959. "Capillary Continuity or Discontinuity in Cement Paste." *PCA Bullentin* 10: 2–12.
- Rahman, Mohammad, Ahmed Ibrahim, and Riyadh Hindi. 2020. *Bridge Decks: Mitigation of Cracking and Increased Durability—Phase III*. Rantoul, IL: Illinois Center for Transportation. <https://doi.org/10.36501/0197-9191/20-022>
- De Rooij, Mario, Kim Van Tittelboom, Nele De Belie, and Erik Schlangen. 2013. *Self-Healing Phenomena in Cement-Based Materials: State-of-the-Art Report of RILEM Technical Committee 221-SHC*. Dordrecht: Springer.
- Sabir, B. B., S. Wild, and M. O'Farrell. 1998. "A Water Sorptivity Test for Martar and Concrete." *Materials and Structures* 31 (8): 568.
- Sisomphon, K., and O. Copuroglu. 2010. "Some Characteristics of a Self Healing Mortar Incorporating Calcium Sulfo-Aluminate Based Agent." In *Proceedings of the 2nd International Conference on Durability of Concrete Structures*, 157–64.
- Wang, Li-Cheng. 2009. "Analytical Methods for Prediction of Water Absorption in Cement-Based Material." *China Ocean Engineering* 23 (4): 719–28.
- Yang, Zhifu, W. Jason Weiss, and Jan Olek. 2006. "Water Transport in Concrete Damaged by Tensile Loading and Freeze–Thaw Cycling." *Journal of Materials in Civil Engineering* 18 (3): 424–34.



I ILLINOIS